St. John's University

St. John's Scholar

Theses and Dissertations

2023

OVEREXPRESSION OF ABCC1 AND ABCG2 CONFERS RESISTANCE TO BMN-673, A POLY (ADP-RIBOSE) POLYMERASE (PARP) INHIBITORS

Qiuxu Teng

OVEREXPRESSION OF ABCC1 AND ABCG2 CONFERS RESISTANCE TO

BMN-673, A POLY (ADP-RIBOSE) POLYMERASE (PARP) INHIBITORS

A dissertation submitted in partial fulfillment
of the requirements for the degree of

DOCTOR OF PHILOSOPHY

to the faculty of the

DEPARTMENT OF PHARMACEUTICAL SCIENCES

of

COLLEGE OF PHARMACY AND HEALTH SCIENCES

at

ST. JOHN'S UNIVERSITY
New York
by
Qiuxu Teng

Date Submitted 12/10/2022   Date Approved 12/30/2022

_____   _____

Qiuxu Teng   Dr. John N.D. Wurpel

ABSTRACT

OVEREXPRESSION OF ABCC1 AND ABCG2 CONFERS RESISTANCE TO

BMN-673, A POLY (ADP-RIBOSE) POLYMERASE (PARP) INHIBITORS

Qiuxu Teng

Cancer remains a growing public health challenge worldwide. Although the development of chemotherapies has effectively reduced the cancer death rate and improved patients' prognosis, the frequent occurrence of multi-drug resistance (MDR) in cancer has caused impairments on the efficacy of many structure-unrelated anticancer agents, leading to treatment failure and recurrence. One of the most common causes of MDR is the overexpression of ATP-binding cassette (ABC) transporters on cancer cell membranes, which transport anticancer drugs out of cancer cells, thereby reducing the intracellular drug concentration. BMN-673 (talazoparib) is a potent poly (ADP-ribose) polymerase (PARP) inhibitor that is approved for BRCA-mutated HER2-negative locally advanced or metastatic breast cancer and is under clinical investigations for treating other solid tumors. The present study aims to explore the role of ABCC1 and ABCG2 transporters in regulating the efficacy of BMN-673 in ovarian cancer. The cell viability tests indicated that the effect of BMN-673 is limited in both drug-selected or gene-transfected cell lines overexpressing ABCC1 or ABCG2. The known ABCC1 inhibitor, ONO-1078, and ABCG2 inhibitor, cabozantinib, can sensitize ABCC1- or ABCG2-overexpressing cells to BMN-673. The computational molecular docking analysis suggested that BMN-673 interacts with the drug-binding pocket of ABCC1 or ABCG2. In mechanism-based studies, BMN-673 shows a competitive inhibition on the substrate drug efflux activity of ABCC1 or ABCG2. To further investigate the mechanism of BMN-673 resistance in ovarian cancer,

the BMN-673-resistant subline A2780/T4 was constructed from human ovarian cancer cell line A2780 by drug selection with gradually increasing concentration. The upregulated ABCC1 and ABCG2 protein expression were observed on the plasma membrane of A2780/T4 cells, resulting in enhanced resistance to other ABCC1 or ABCG2 substrate drugs. Furthermore, the knockout of either ABCC1 or ABCG2 gene can increase sensitivity to BMN-673 in the A2780/T4 subline. Consistently, observations from in vivo experiments showed that the same drug-resistant characteristics could be retained in the tumor xenograft mice models. Taken together, BMN-673 is an MDR-susceptible agent due to its interactions with ABCC1 or ABCG2, and overexpression of ABCC1 or ABCG2 transporter may attenuate its therapeutic effect in cancer cells.

ACKNOWLEDGEMENTS

TABLE OF CONTENTS

LIST OF TABLES

LIST OF FIGURES

CHAPTER 1
INTRODUCTION

1.1 Cancer Statistics

The occurrence of cancer has increased due to population growth and aging, and the increasing prevalence of established risk factors such as smoking, physical inactivity, overweight, and changes in reproductive patterns (including lower parity and later age at first birth) associated with economic development and urbanization [1]. Although the cancer incidence rate and the death rate have declined during the past decade, cancer is still the second leading cause of death in the United States. The three most common cancers are prostate, lung, and colorectal cancers in men, and breast, lung, and colorectum cancers in women, which are also the most common causes of cancer death [2]. Only surpassed by accidents, cancer is also the second most common cause of death among children between 1 to 14 years old. One-tenth of the children diagnosed with cancer will die each year. Cancers in adolescents (15 to 19 years) show different conditions based on cancer types and distribution from children [3, 4].

1.2 Multi-drug Resistance

Multi-drug resistance (MDR) is defined as the resistance of cancer cells to multiple chemotherapeutic drugs with different structures and mechanisms of action [5, 6]. Therefore, resistance is a significant factor in the failure of cancer chemotherapy, although various drugs can be used for anticancer actions [7]. Chemotherapiesbecame ineffective due to endogenous MDR of cancer cells or MDR acquisition during chemotherapy [6, 8], leading to refractory cancer and tumor recurrence, which contributes to increasing cancer-related death.

The mechanisms of MDR are classified in seven categories: (1) overexpression of ATP-binding cassette (ABC) transporters as the leading primary membrane transporters, which could increase drug efflux [9]; (2) dysfunction of influx transporters such as solute carriers, which could decrease drug uptake [10]; (3) physiological metabolic enzymes, for example, glutathione S-transferase and cytochrome P450 enzymes which promote drug metabolism hence increasing elimination of anticancer drugs [11, 12]; (4) epigenetic regulation and microRNA regulation that could be carried out simultaneously by the cancer cells to elevate adaptablity [13, 14]; (5) changes in the expression level of B cell lymphoma (BCL) family proteins or mutations in the p53 pathway which blocks apoptotic signaling pathways [15, 16]; (6) mutation of drug target or activation of other targets and signaling pathways by feedback of anticancer drugs [17]; and (7) chemotherapy resistance resulting from changes in the microenvironment, such as hypoxia and cancer stem cell regulation [18, 19]. (Figure 1.) Cellular-based MDR mechanisms are further divided into transporter-based classical MDR phenotypes and non-classical MDR phenotypes [20].
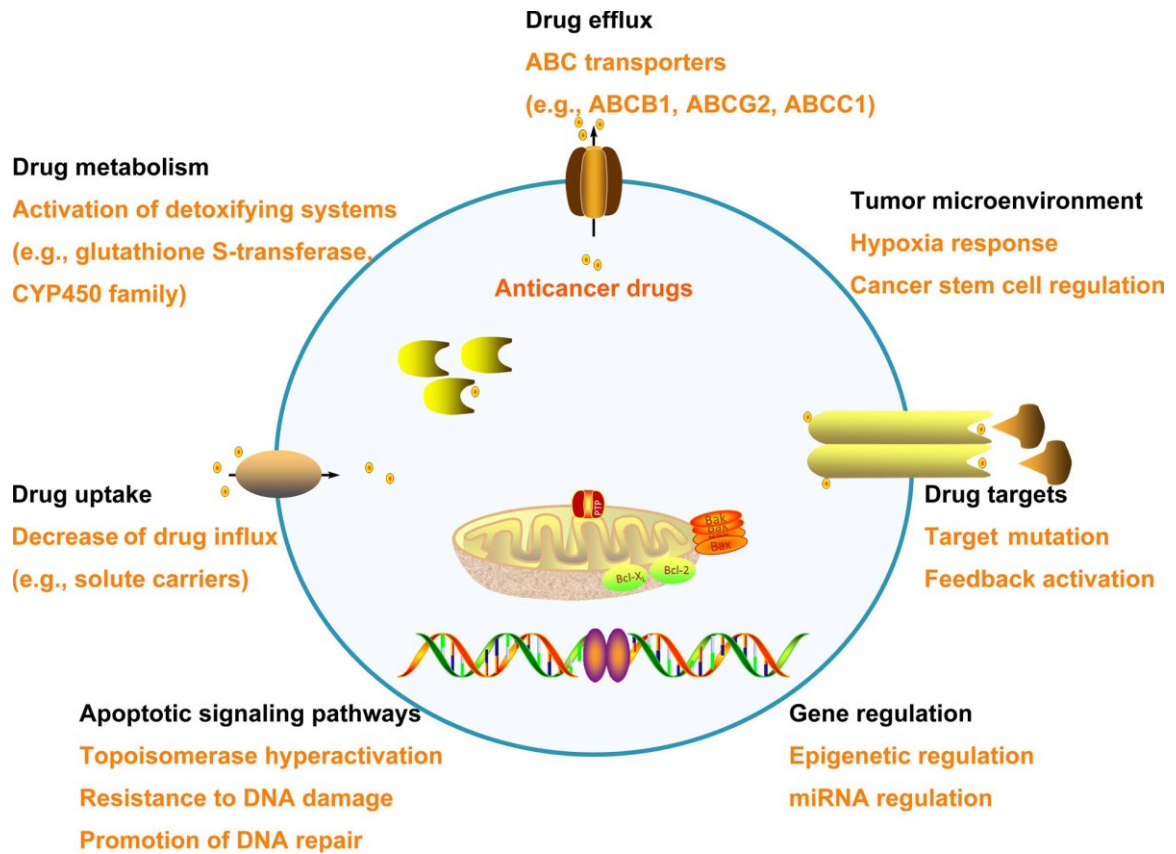
Figure 1. Complicated mechanisms of multi-drug resistance (MDR) in cancer. (Adapted from [20])

1.3 ATP-binding Cassette Transporter

The ATP-binding cassette (ABC) protein superfamily consists of 49 members classified into seven subfamilies from A to G based on their sequence similarities and structure organization [21]. The ABC transporters hydrolyze ATP to transport substrates across the cell membrane against its electrochemical gradient. Many human ABC proteins, including ABCB1 (P-glycoprotein(P-gp), multi-drug resistance 1 (MDR1) protein), ABCG2 (breast cancer resistance protein (BCRP)), and ABCC1 (multi-drug resistance-associated protein 1 (MRP1)), are efflux protein transporters [6]. This decrease in the intracellular accumulation of chemotherapeutic drugs is one of the most common causes

of MDR. Human ABCB1 is the first identified ABC transporter of which overexpression could induce the resistance of cancer cells to a series of chemotherapeutic drugs [6]. The ABCG2 transporter is usually overexpressed in breast, ovarian, lung, gastric, and colon cancer [6]. Moreover, much evidence has shown that the ABCC1 transporter also leads to resistance of cancer cells [6]. The ABC transporter has been recognized as the culprit in the development of MDR. Current strategies to overcome MDR mainly focus on continuing the development of reversal agents to inhibit or inactivate ABC transporters to increase the concentration of intracellular anticancer drugs [6, 20].

1.3.1 ABCB1

ABCB1 is a 170 kDa membrane transporter ubiquitously expressed in the kidney, intestine, brain, and placenta. It could transport several chemotherapeutic drugs like paclitaxel, doxorubicin, and vincristine out of the cancer cells. ABCB1 consists of two nucleotide-binding domains (NBD1 and NBD2) for ATP binding and hydrolysis and two transmembrane-binding domains (TMD1 and TMD2) forming a drug-binding pocket that contributes to drug efflux [22]. Clinical applications of the combination with ABCB1 modulators and anticancer drugs have been recognized as a promising strategy to circumvent ABCB1-mediated efflux for an extended period. Three generations of ABCB1 inhibitors and other compounds have been developed over the past few decades. Verapamil is one of the first generations of these MDR reversal agents [23], which is used as a calcium channel blocker. However, the *in vivo* effective concentration for reversal is too high to achieve safely [24], and the dose of verapamil required is much higher than clinically relevant doses, making it likely to cause toxic reactions in almost all patients. This led to

limited clinical application as a reversal agent. Although the second generation of ABCB1 inhibitors are synthesized around the first-generation pharmacophores to increase the affinity to P-gp while reducing dose-limiting toxicity, and the third generation is specifically designed to have high affinity for P-gp and low pharmacokinetic interactions [25], none of developed inhibitors were approved for use in the market due to lack of significant clinical efficacy, or concerns about their safety.

1.3.2 ABCG2

ABCG2 is a half transporter consisting of 655 amino acids and was first identified in the multi-drug resistant human breast cancer cell line MCF-7/AdrVp [26, 27]. It is a 72 kDa plasma membrane transporter with a broad expression on the apical surface of the small intestine, canalicular liver membrane, colon epithelium, and placental syncytiotrophoblasts. ABCG2 transporters confer MDR by increasing efflux, thus reducing the intracellular accumulation of a broad spectrum of chemotherapeutic agents, including mitoxantrone, methotrexate, flavopiridol, topoisomerase I inhibitors like topotecan, irinotecan and its active metabolite SN-38, and kinase inhibitors such as gefitinib and imatinib [28]. Recent clinical studies have shown that the overexpression of ABCG2 in adult and childhood leukemia results in poor prognosis[29]. Another study suggested that ABCG2 may play a role in MDR in non-small cell lung cancer (NSCLC) by finding high levels of intrinsic ABCG2 mRNA expression in NSCLC tumor samples [30]. Many previous studies have been conducted to design potential modulators to overcome ABCG2-mediated MDR [31]. Fumitremorgin C (FTC) isolated from Aspergillus fumigatus is a highly efficient and specific ABCG2 inhibitor. However, due to its neurotoxicity, it is not

suitable for therapeutic use [32, 33]. Estrogens like estrone and 17β-estradiol [34] and novobiocin, a coumermycin antibiotic [35], all failed to show ABCG2 inhibitory capacity *in vivo* albeit promising results *in vitro*. Cabozantinib (CBZ) is a small molecule tyrosine-kinase receptor inhibitor, which could also inhibit the ABCG2 transporter function [36]. The reversal capability of CBZ could be extended from *in vitro* cell model to *in vivo* xenograft model, which is considered a potential approach to overcoming ABCG2-mediated MDR [37].

1.3.3 ABCC1

The human ABCC1 spans over 194 kb on human chromosome 16p13.1 [38], which is not only expressed in drug-resistant cancer cells but also widely expressed in normal tissues, including those critical for drug absorption (lung and intestine), metabolism and clearance (liver and kidney), and barrier sites (blood-brain barrier and maternal-fetal barrier or placenta) [39, 40]. ABCC1 and six other ABCC proteins have five distinct domains with two NBDs and 17 transmembrane alpha helices distributed over three TMDs [40, 41]. Substrates for ABCC1 are commonly neutral and anionic hydrophobic natural products. In particular, ABCC1 also transports glutathione (GSH) which has a variety of physiological functions and pathophysiological events such as inflammatory response and oxidative stress due to its special transport properties [42]. Furthermore, ABCC1 transporters sometimes use GSH for the transport of xenobiotics, including antineoplastic drugs such as vincristine [43] and doxorubicin [44], and drugs that bind to glutathione, glucuronide, or sulfate [45]. ABCC1 was first discovered in a multi-drug resistant small-cell lung cancer cell line [46], and later overexpression of ABCC1was found in various

hematological and solid tumors [40]. Like other ABC transporters, ABCC1 is mainly localized on the cytoplasm membrane of cancer cells, suggesting its transport role in the clinical drug resistance [40]. The crystal structure and transport mechanisms of ABCC1 are still elusive, although a comprehensive study of ABCC1 has been carried out. Moreover, the widespread presence of splice variants and mutations in ABCC1 in cancer also makes their function unpredictable [47]. Tissue-specific expression patterns and extensive genetic variations make ABCC1 the best candidate for markers or members of multi-label panels for predicting chemoresistance [48].

1.4 Poly(ADP-ribose) polymerases (PARP) and Ovarian Cancer

Poly (ADP-ribose) polymerase (PARP) is a protein family responsible for DNA damage detection and signal transduction [49, 50]. PARP inhibitor is a class of targeted drugs approved in recent years for cancer treatment, which can interact with the binding site of the PARP cofactor (NAD+) and trap PARP on DNA [51]. Genetic complexity and DNA damage repair defects are common in different cancer types and can induce tumor-specific vulnerabilities [52, 53]. PARP inhibitors exploit defects in the DNA repair pathway through synthetic lethality. They have emerged as promising anticancer therapies, especially in cells containing deleterious germline or somatic breast cancer susceptibility protein (BRCA)-mutated tumors [54].

PARPs are involved in various DNA repair activities, including DNA repair and maintenance of genome integrity, DNA methylation, induction of apoptosis [55], programmed cell death, transcriptional regulation, and metabolic regulations [52, 56]. The PARP enzymes family has 17 members, including PARP1, PARP2, PARP3, PARP5a, and

PARP5b. PARP1 is the most important member and the most studied enzyme, with great significance in DNA repair [57]. PARP proteins have a unique poly ADP-ribosylation (PARylation) function, a post-translational modification involving the addition of poly (ADP-ribose) to nucleoproteins [58, 59]. PARP detects DNA damage and helps select repair pathways [60]. In particular, PARP is involved in DNA single-strand break (SSB) and base excision repair (BER) pathways [59, 61]. Breaks in DNA strands trigger PARP activity, and when PARP detects SSB, it binds to DNA, undergoes a structural change, then begins to synthesize poly-ADP-ribose (PAR) chains that serve as signals for other DNA repair enzymes [62]. Cleavage of NAD+ substrates by releasing nicotinamide is required to generate ADP-ribomonomers. Furthermore, PARP can act on the double-strand break (DSB) repair pathway through the regulatory enzymes MRE11 and NBS1 [63], which is a crucial factor in another important pathway of DNA repair, namely homologous recombination (HR) [64, 65]. It has been hypothesized that SSB persists when PARP function is impaired, resulting in DSB during replication [66]; this DSB is usually repaired by homologous recombination repair (HRR), which allows replication to continue [66]. However, loss of PARP activity becomes lethal when HRR is compromised. PARP inhibitors are oral small molecule inhibitors that play a crucial role in repairing DNA SSBs via BER way. PARP inhibition in BRCA-mutated tumor cells induces synthetic lethality, which results from the simultaneous targeting of two DNA repair pathways resulting in profound cytotoxicity on tumor cells without affecting normal cells [67]. In 1997, Hartwell and colleagues first proposed using synthetic lethality as a potential strategy for cancer therapy [68]. From this perspective, the PARP inhibitor was found and designed. The synthetic lethality of PARP inhibitor is directed against BRCA-mutated or HR-deficient

tumors [69]. BRCA1 and BRCA2 are essential tumor suppressor genes that repair DNA DSBs through the HR repair pathway [70]. The synthetic lethality phenomenon has been well documented by deleterious mutations in BRCA1 and BRCA2 [71, 72]. The repair of strand breaks (SSBs) and promotion of the formation of double-strand breaks (DSBs) have been of interest [73]. As noted above, alternative repair pathways are activated in cases where the canonical repair pathway is deficient, for example, BRCA failure. At this point, the activity of PARP becomes more critical to the organism. Since BRCA mutant cells lack HR repair machinery, simultaneous inhibition of PARP -induced DNA repair can lead to cell death through apoptosis. DNA repair inhibition by a PARP inhibitor in damaged tumor cells can lead to tumor cell death by increasing genomic instability [71]. Traditionally, PARP inhibition has been thought to be primarily associated with DNA damage and its downstream effects, apoptosis, which is lethal to cancer cells with defective HR pathways such as BRCA1/2 mutations [74-76]. However, the mechanism of PARP inhibition in cancer cells is not fully understood, and whether it can suppress tumors through mechanisms additional to DNA damage remains unknown. Furthermore, PARP inhibitor is also designed to interact with chemotherapy or radiotherapy by blocking the repair of DNA damage caused by chemotherapy or radiotherapy [77-80].The first PARP inhibitor, Olaparib, was approved in 2014? and can interact with the NAD+ binding site located in the catalytic domain of PARP [55, 81]. In addition to directly inhibiting the repair activity of PARP by competing with NAD+ binding, PARP inhibitors, including rucaparib, olaparib, niraparib, and BMN-673 (talazoparib), can also trap PARP1 at the SSB level, thereby preventing DNA repair [82]. PARP1 capture underlies PARP inhibitor cytotoxicity [82], and the pharmacodynamic differences between the clinically used PARP inhibitors

are precise because of the ability to capture PARP1. BMN-673 was the most potent one, which could capture PARP1 about one hundred times more efficiently than niraparib.

BMN 673 is a novel, potent, and selective inhibitor of PARP1/2 (PARP1 IC50: 0.57 nM). It achieves antitumor cell responses and elicits DNA repair markers at a much lower concentration compared to previous generation PARP1/2 inhibitors [58, 83], effectively against BRCA1/2 and PTEN mutant cancers in preclinical models. Its molecular formula is $C_{19}H_{14}F_2N_6O$, and its molecular weight is 380.359 g/mol. The chemical structure of BMN-673 is shown in Figure 2. BMN-673 is a potent oral PARP1/2 inhibitor with catalytic activity similar to olaparib and rucaparib; plays an essential role in detecting and repairing single-stranded DNA damage but, in contrast, does better in capturing PARP-DNA at the site of DNA damage [84]. BMN-673 was generally well tolerated and distributed in tissues, exhibited an excellent PK profile, and had good oral bioavailability [83]. In addition to inhibiting PARP catalytic activity, BMN-673 is currently the most potent PARP1/2 inhibitor *in vitro*, based on its enhanced ability to trap PARP on DNA and its subsequent higher cytotoxicity [84, 85]. PARP inhibitors differ in their catalytic inhibition potency and ability to capture PARP, which is related to their size, structure, and allosteric differences in the NAD+ binding sites. In this regard, BMN-673 had the greatest *in vitro* cytotoxicity and PARP capture ability [86], followed by niraparib, and veliparib was the weakest [82, 87]. BMN-673 inhibits PARP catalytic activity, trapping PARP1 on damaged DNA and causing cell death in BRCA1/2 mutant cells [83]. Compared to other PARP inhibitors, BMN-673 has a more vital stereospecific PARP-DNA capture ability and can enhance the toxic cellular effects of temozolomide, carboplatin, and the active metabolites of irinotecan, SN-38 [85, 86]. The side effects of BMN-673 are more

like those of traditional chemotherapy drugs compared to other clinically approved PARP inhibitors [54]. This results in significant differences in doses between PARP inhibitors [88].
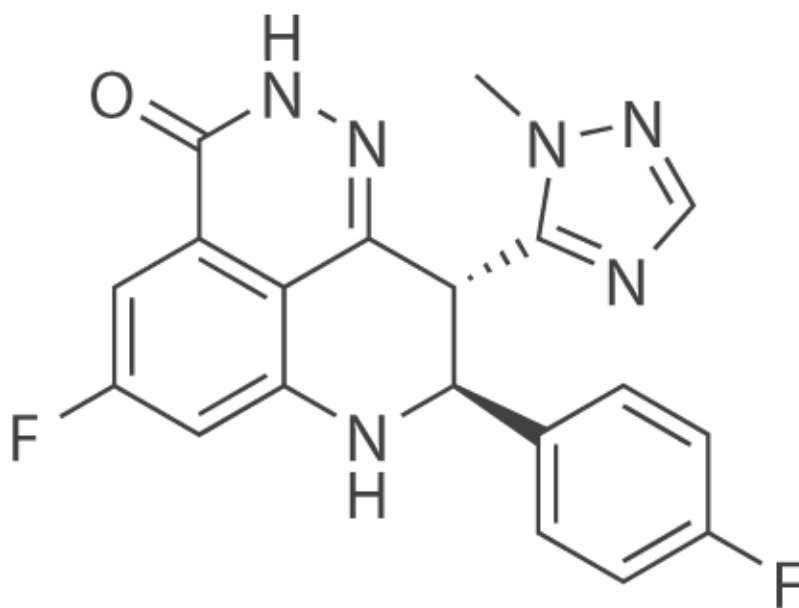
Figure 2. The chemical structure of BMN-673.

Ovarian cancer is one of the most common malignant tumors of the female reproductive tract, ranking third after cervical and uterine cancer. Ovarian cancer is the most lethal gynecological malignancy, and the mortality rate ranks first among malignant tumors of the female reproductive system [89]. Approximately 70% of patients are initially diagnosed with advanced or metastatic disease [90, 91]. The long-established primary treatment for ovarian cancer consists of surgical cytoreduction followed by platinum-based chemotherapy. Unfortunately, this treatment is associated with a high frequency of early relapses. The recurrent disease requires further chemotherapy, but few patients are cured.

PARP inhibitors have shown promising activity against ovarian cancer [92]. While only 15-20% of ovarian cancers harbor germline or somatic mutations in BRCA1 or BRCA2, approximately 30-50% have defects in HR DNA repair. Cells deficient in HR repair depend on alternative DNA repair pathways for survival, which provides a potential target for DNA-damaging agents. PARP is essential in detecting DNA SSB and mediating DNA repair through HR-replenished pathways [92]. In HR-deficient cancer cells, inhibition of PARP leads to the accumulation of DNA DSB and cell death. The development of PARP inhibitors has transformed how ovarian cancer patients are treated [93], and containing a PARP inhibitor in chemotherapeutic regimens has become a primary therapeutic strategy to treat BRCA-mutated ovarian cancer [94] and HR-deficient advanced ovarian cancer [95]. The PARP inhibitors provide tremendous clinical benefit to ovarian cancer patients [96]. Olaparib, the most classic and potent PARP inhibitor, has been approved by the US FDA for the treatment and maintenance of advanced ovarian cancer with germline BRCA1/2 mutations [74, 97, 98] and remains the only approved drug. Furthermore, the remarkable efficacy of PARP inhibitor use in ovarian cancer is not limited to patients with germline BRCA1/2 mutations but extends to patients with tumors defective in HR repair pathways [99].BRCA1/2 mutations remain the most potent genetic marker of the sensitivity to PARP inhibitors [90]. However, 40-70% of BRCA1/2-mutant ovarian cancers do not respond to PARP inhibitors [91, 100]. Drug resistance has become a major obstacle for PARP inhibitor applications.

As more and more PARP inhibitors have entered clinical trials as potential cancer targeted therapy and potential drug candidates have often received multiple chemotherapy regimens, there is an urgent need to study resistance mechanisms when considering the

administration of PARP inhibitors. It has been found that insufficient amount of functional PARP1 may account for a limited tumor response to PARP inhibitors because PARP1 is required for the cytotoxicity of PARP1-trapped substrates and PARP inhibitors. Besides, increased expression of the ATP-dependent efflux pump ABCB1, which encodes the membrane drug efflux transporter P-glycoprotein, may readily efflux PARP inhibitors out of tumor cells and lead to resistance to the PARP inhibitors olaparib or rucaparib but is not for the resistance to either veliparib or AZD2461 [101, 102]. However, this resistance can be reversed with the ABCB1 inhibitors verapamil, elacridar, and tariquidar [103].

CHAPTER 2
MATERIALS AND METHODS

2.1 Chemicals and reagents

BMN-673, cabozantinib, and topotecan were purchased from ChemieTek (Indianapolis, IN). Dulbecco's modified Eagle's medium (DMEM), fetal bovine serum (FBS), bovine calf serum (BS), penicillin/streptomycin, and trypsin 0.25% were purchased from Hyclone (GE Healthcare Life Sciences, Pittsburgh, PA). A 10X solution of phosphate-buffered saline (PBS), Alexa Fluor 488 conjugated rabbit anti-mouse IgG secondary antibody, Alexa Fluor 488 conjugated goat anti-rabbit IgG secondary antibody, 4′,6-diamidino-2-phenylindole (DAPI), and novobiocin were purchased from Thermo Fisher Scientific Inc. (Rockford, IL). The MRP1/ABCC1 (D5C1X) Rabbit mAb and HRP conjugated secondary antibody were purchased from Cell Signaling (Danvers, MA), and the anti-BCRP antibody (BXP-21) was purchased from Millipore-Sigma (Burlington, MA). The monoclonal anti-P-glycoprotein (MDR) antibody produced in mouse, paclitaxel, vincristine, vinblastine, colchicine, cepharanthine, 3-(4, 5-dimethylthiazol-yl)-2, 5-diphenyltetrazolium bromide (MTT), dimethyl sulfoxide (DMSO), and Triton X-100, were obtained from Sigma Chemical Co. (St. Louis, MO). Mitoxantrone, cisplatin, Ko143, and MK-571 were obtained from Enzo Life Sciences (Farmingdale, NY). [^{3}H]-paclitaxel ([^{3}H]-PTX) (15 Ci/mmol) and [^{3}H]-vincristine ([^{3}H]-VCR) (0.7 Ci/mmol) were purchased from Moravek Biochemicals (Brea, CA). Liquid scintillation cocktail was a product of MP Biomedicals, Inc (St. Ana, CA). All other chemicals were purchased from Sigma Chemical Co (St. Louis, MO).

2.2 Cell lines and cell culture

The human epidermal carcinoma cell line KB-3-1 and its drug-resistant ABCB1-overexpressing KB-C2 cells were cloned from KB-3-1 and maintained in the medium with 2 mg/mL of colchicine, the drug-resistant ABCC1-overexpressing cell line KB-CV60, maintained in medium with 1 µg/mL of cepharanthine and 60 ng/mL of vincristine, were used in this study [104]. The topotecan-induced ABCG2-overexpressing human non-small cell lung cancer (NSCLC) cell line NCI-H460/TPT10 was maintained with 10 µM topotecan [105], and its drug-sensitive NCI-H460 cell lines were also used in this project. HEK293/pcDNA3.1, HEK293/ABCB1, and HEK293/ABCC1 cells lines were established by transfecting HEK293 cells with either the empty pcDNA3.1 vector or the vector containing full-length *ABCB1* (HEK293/ABCB1), or *ABCC1* (HEK293/ABCC1), or three phenotypes of *ABCG2* (HEK293/ABCG2-R2, HEK293/ABCG2-G2, and HEK293/ABCG2-T7) DNA, respectively, and were cultured in medium containing 2 mg/mL of G418 (Enzo Life Sciences, Farmingdale, NY) [106]. Human ovarian cancer cell line A2780 was used to construct BMN-673-resistant subline A2780/T4 with the final selection concentration of 4 µM BMN-673. Only A2780 and A2780/T4 were cultured in RPMI1640 medium, and all the other cell lines were cultured in DMEM medium with 10% FBS and 1% penicillin/streptomycin at 37 °C with 5% CO_2. All drug-resistant cell lines were grown in a drug-free culture medium for more than two weeks before their use.

2.3 Cell cytotoxicity determined by MTT assay

As previously described [107], an MTT assay was used to examine the cell viability rate after treatment with BMN-673 and other chemotherapeutic drugs. Briefly, 5×10^3-

7×10^3 cells/well were evenly seeded into a 96-well plate. The next day, serial concentrations of substrate drugs were added to designated wells with or without 2 h pretreatment of known ABCC1 or ABCG2 inhibitors at indicated concentrations. After a 68 h incubation period, an MTT solution was added following 4 h incubation at 37°C in the dark. The supernatant was discarded, and this was followed by the addition of DMSO to dissolve the resulting formazan crystals. The absorbance was measured at 570 nm using a UV/Vis microplate spectrophotometer (Fisher Sci. Fair Lawn, NJ). MK-571 and ONO-1078 were used as positive control reversal agents for ABCC1-overexpressing cell lines in this assay. At the same time, Ko143 and cabozantinib were used as the positive control reversal agents for ABCG2-overexpressing cell lines. Resistance fold (RF) was calculated by dividing the IC_{50} values for antineoplastic drugs of drug-sensitive cells without inhibitors by the IC_{50} values for chemotherapeutic drugs of drug-sensitive cells with inhibitors or drug-resistant cells with or without inhibitors.

2.4 Molecular docking of BMN-673 with ABCC2 and ABCG2 models

As previously described, the BMN-673 3-D structure was constructed for docking simulation with the ABCC1 or ABCG2 model [108]. Substrate-bound ABCC1 (PDB ID: 5UJA) and ABCG2 (PDB ID: 6VXI) were obtained from RCSB Protein Data Bank. Both models are inward-facing with resolutions of 3.3 Å (ABCC1) [109] and 3.7 Å (ABCG2) [110]. Docking calculations were performed in AutoDock Vina (version 1.1.2) [111]. Hydrogen atoms and partial charges were added using AutoDockTools (ADT, version 1.5.4). Docking grid center coordinates were determined from the bound ligand substrate provided in 5UJA PDB files. Receptor/ligand preparation and docking simulation were

performed using default settings. The top-scoring pose (sorted by affinity score with the unit of kcal/mol) was selected for further analysis and visualization.

2.5 Accumulation and efflux assay

Tritium-labeled vincristine or mitoxantrone accumulation assay was performed to assess the transport function mediated by MDR-associated ABC transporters [107]. Each cell line was seeded evenly into a 24-well plate with a density of 1×106 cells/well for the accumulation assay. The next day, cells were pretreated for 2 h with or without BMN-673 or positive ABCC1 or ABCG2 inhibitor at indicated concentrations. After that, the medium was replaced by medium containing 5 μM [^{3}H]-vincristine ([^{3}H]-VCR) for ABCC1 or [^{3}H]-mitoxantrone ([^{3}H]-MX) for ABCG2 and with BMN-673 or the reversal agents, respectively. After 2 h incubation, the medium was discarded, and the cells were washed with ice-cold PBS three times, lysed, and then transferred to the scintillation fluid. For the efflux assay, similar procedures were performed as the accumulation assay. After discarding the medium containing [^{3}H]-VCR and [^{3}H]-MX, the cells were washed with ice-cold PBS and incubated with medium in the presence of BMN-673 or the reversal agents. The cells were washed three times, lysed, and then transferred to the scintillation fluid at different time points of 30, 60, and 120 min, respectively. Radioactivity was measured using the Packard TRI-CARB1 190`A liquid scintillation analyzer (Packard Instrument, Downers Grove, IL).

2.6 Establishment of a BMN-673 resistant A2780 cell line

The BMN-673 resistant cell line, A2780/T4, was generated by continuously maintaining A2780 cells in a complete culture medium containing BMN-673 in gradually increasing concentrations. To be detailed, the parental A2780 cells were first cultured in RPMI1640 with 0.1 μM BMN-673 at 37°C for 72 h, then replaced with fresh drug-free medium. The remaining cells were passaged and cultured in medium containing 0.1 μM BMN-673 until they stabilized. The concentration of BMN-673 was increased stepwise up to 4 μM, with a total of 6 months of culturing. The established A2780/T4 cells were cultured in the BMN-673-free medium for 12 weeks prior to further experiment.

2.7 Western blotting analysis

Using an established protocol, a Western blot was conducted to determine protein expression level [107]. After treatment with the indicated concentration of BMN-673 for 72 h in A2780 and A2780/T4 cells, cells were incubated with a lysis buffer (2.5% 1M Tris, 0.15% EDTA, 1% sodium deoxycholate, 0.1% SDS, 0.88% NaCl, 1% Triton-X and protease inhibitor cocktail) on ice for 20 min, followed by centrifugation at 12,000g at 4 °C for 20 min. The supernatant was collected, and the protein concentration was determined by a bicinchoninic acid (BCA)-based protein assay (Thermo Scientific, Rockford, IL). Equal amounts of total protein (20–30 μg) samples were separated by SDS-polyacrylamide gel electrophoresis and transferred to a polyvinylidene difluoride (PVDF) membrane. After being blocked by 5% BSA within TBST (Tris-buffered saline, 0.1% Tween 20) for 2 h at room temperature, the membrane was incubated with primary antibody MRP1 (1:1000, detects ABCC1) or BCRP (1:1000, detects ABCG2) overnight at 4 °C. The next day, after

washing with TBST, the membrane was incubated with an HRP-conjugated secondary antibody for 2 h at room temperature. Subsequently, the chemiluminescence signal of the protein antibody complex was visualized by ECL substrate as per the manufacturer's instructions. The relative density of each protein band was analyzed by ImageJ software (NIH, Bethesda, MD, USA).

2.8 Immunofluorescence assay

A2780 and A2780/T4 cells were seeded at a density of 1×10^4 cells/well in 24-well plates and cultured at 37 °C for 24 h, followed by incubation with indicated concentrations of BMN-673 for 72 h, respectively. Then, cells were washed twice with ice-cold PBS, followed by fixation using 4% paraformaldehyde, permeabilization using 0.25% Triton X-100, and cells were incubated with BSA (6% with PBS) for 1 h followed by primary antibody MRP1 (1:1000, detects ABCC1) or BCRP (1:1000, detects ABCG2) overnight at 4°C. Cells were further incubated with Alexa Fluor 488 conjugated IgG secondary antibody (anti-rabbit for ABCC1, 1:1000; or anti-mouse for ABCG2, 1:1000) for 1 h in the dark. DAPI solution was used to counterstain the nuclei. Immunofluorescence images were taken with an EVOS FL Auto Imaging System (Thermo Fisher Scientific Inc., Rockford, IL, United States).

2.9 Intracellular accumulation of BMN-673 determined by HPLC assay

The HPLC assay was carried out with a modified protocol as previously described [112]. Briefly, both A2780 and A2780/T4 cells were seeded in six-well plates (1×10^6 cells per well) and incubated overnight. The following day, cells were pre-treated with or

without ABCC1 inhibitor ONO-1078 or ABCG2 inhibitor cabozantinib for 2 h. Subsequently, cells were further incubated with BMN-673 in the presence or absence of inhibitors for another 2 h. In the end, cells were harvested and subjected to HPLC analysis.

2.10 Construction of A2780/T4-ABCC1 or -ABCG2 knockout cell line

The ABCC1 or ABCG2 gene knockout subline of A2780 was constructed using a clustered regularly interspaced short palindromic repeats (CRISPR)/CRISPR-associated (Cas) 9 system. The custom-designed mammalian CRISPR vector and its control vector were purchased from VectorBuilder Inc. (Chicago, IL, United States). The vector consists of a U6 promoter that regulates the transcription of guide RNA (gRNA), a CBh promoter that regulates the expression of Cas9 nuclease, and a CMV promoter that regulates the transcription of the neo gene responsible for resistance to G418. The gRNA of the human *ABCC1* targeting vector contains a specific 20 bp guide sequence of 5'-GTTGACAATCTCCCCGACCG-3', and the human *ABCG2* targeting vector contains a specific 20 bp guide sequence of 5'-GATCATTGTCACAGTCGTAC-3' selected specifically for Cas9 protein. In this study, A2780/T4 cells were transfected with either the targeting vector with *ABCC1* gene or *ABCG2* gene using Fugene6 transfection reagent (Madison, WI, United States) following the manufacturer's protocol. After changing the medium every third day, the transfected cells were incubated with the selection medium for 14 days. Then, single positive colonies were obtained by limited dilution. Protein expression was measured using western blotting to verify the knockout of ABCC1 or ABCG2. The A2780/T4-ABCC1 knockout or A2780/T4-ABCG2 knockout subline was further used in drug sensitivity tests to BMN-673 by MTT assay.

2.11 Experimental animals

Female athymic NCR nude mice (14–16 g, age 4–5 weeks) were used for the tumor xenograft model. The project was conducted following the Animal Welfare Act and other federal statutes. The maintenance of the mice and all the in vivo studies were conducted in the Animal Care Center of St. John's University. The animal study was reviewed and approved by the Institutional Animal Care and Use Committee of St. John's University (Protocol #1989).

2.12 *In vivo* tumor model

The BMN-673-resistant A2780/T4 model and the parental A2780 tumor xenograft model were modified from a previously established tumor xenograft model by Chen's Laboratory [37]. Briefly, 4×10^6 of A2780 cells and 6×10^6 of A2780/T4 cells were injected subcutaneously in the same female nude mice, with A2780 and A2780/T4 in the left and right flank near the armpit, respectively. The mice were randomized into four groups (6 in each group) after the subcutaneous tumors reached a mean diameter of 0.5 cm. Different groups then received various treatments every third day with a total of 6 times: (1) vehicle solution (normal saline) as a negative control by mouth (p.o.); (2) BMN-673 (0.3 mg/kg, p.o.); (3) combination of BMN-673 (0.3 mg/kg, p.o.) and cabozantinib (3 mg/kg, p.o.); and (4) combination of BMN-673 (0.3 mg/kg, i.p.) and ONO-1078 (1 mg/kg, p.o.). Cabozantinib or ONO-1078 was given 1 h before BMN-673 administration. Throughout the study, all mice were weighed, and tumors were measured with a caliper every third day before the treatment. Tumor volumes (V) were calculated as previously described [113]. After the treatment cycle, the mice were euthanized by carbon dioxide, and the tumors were

excised and weighed. The ratio of growth inhibition (IR) was calculated according to the formula: IR = 1 - (Mean tumor weight of experimental group/Mean tumor weight of vehicle control group) × 100% [113].

2.13 HPLC protocol for tumor sample collection

The tumors were homogenized using 10 ml PBS. The homogenized mixture was extracted with 10 ml diethyl ether. The mixture was centrifuged at 4° C at 1500 rpm for 10 minutes, and then the diethyl ether layer was collected. The solvent was evaporated, and the residue was redissolved in a 500 µl acetonitrile: TFA (9:1) mixture. It was incubated on ice for 30 minutes to allow protein precipitation. It was then centrifuged at 15000 rpm at 4° C for 20 minutes. The supernatant was collected and filtered through a 0.2 µm filter into HPLC vials, and then the samples were analyzed using HPLC.

2.14 HPLC method

The Agilent 1260 infinity series was used to analyze the samples. The Agilent C18 column with dimensions 5 µm x 250 x 4.6 mm was used. The solvent system used was A=water (with 0.1% formic acid) and B=acetonitrile (with 0.1% formic acid). The injection volume used was 100 µl and the detector wavelength used was 254 nm. The standard curve was created based on dosage. BMN-673 (34.5 µg/ml, 17.25 µg/ml, 8.625 µg/ml, 4.3125 µg/ml, 2.15625 µg/ml, 1.07813 µg/ml, 0.53906 µg/ml, 0.26953 µg/ml, 0.13476 µg/ml)

2.15 Statistical analysis

All experiments were repeated at least three times, and the result values are presented as mean ± SD. One-way ANOVA followed by Tukey's post hoc test was performed for the *in vitro* studies. Two-way ANOVA followed by Tukey's post hoc test was performed to compare multiple groups with repeated tumor volume measurements in the animal study. Statistical significance was set at $p < 0.05$, and statistical analysis was carried out using GraphPad Prism 8 for macOS (GraphPad Software, La Jolla, CA, United States).

CHAPTER 3
RESULTS

3.1 Antineoplastic efficacy of BMN-673 was compromised by the presence of ABCC1 and ABCG2

An MTT assay was performed to examine the susceptibility of BMN-673 to MDR mediated by ABCC1 or ABCG2. Herein, RF value was used to evaluate the degree of increased resistance to BMN-673 resulting from the presence of ABCC1 or ABCG2 transporter. In the preliminary screening, the KB/CV60 cells overexpressing ABCC1 showed resistance to BMN-673 compared to the parental KB-3-1 cells, while ABCB1 overexpressing KB-C2 did not exhibit this kind of resistance (Figure 3). At the same time, drug-induced ABCG2 overexpressing cancer cells also show resistance to BMN-673 (Figure 4). In addition, the cytotoxicity of BMN-673 has also been tested in ABCC1-overexpressing HEK293 cells and the vector control cells. Vincristine and vinblastine, the substrates of ABCC1, were used as positive controls, while cisplatin, which is not transported by ABCC1, was used as a negative control. Also, cells transfected with wild-type (R482) or mutant (R482T or R482G) ABCG2 were used. In this assay, topotecan and mitoxantrone, known substrates of ABCG2 used as positive controls, while cisplatin, which is not transported by ABCG2 used as the negative control. Resistance to mitoxantrone and topotecan was observed in both drug-induced resistant cells and transfected cells. As cisplatin is not an ABCG2 substrate, the IC_{50} values were similar between the resistant and the parental cells.

BMN-673 has similar resistance in the ABCC1 overexpressing cells as vincristine and vinblastine, which indicates that BMN-673 might be a substrate of ABCC1. While BMN-673 has reduced toxicity to H460/TPT10 cells compared to the parental H460, the

IC$_{50}$ from S1 and S1-M1-80 cells were similar (Figure 7). This indicated that BMN-673 might be a substrate of wildtype ABCG2 specifically but not a substrate of mutant ABCG2. The same trend was observed in the transfected ABCG2 overexpressing HEK293 cell (Figure 8). Both mitoxantrone and topotecan showed resistance in all three transfected ABCG2 overexpressing cells compared to the vector control cells. In contrast, BMN-673 only showed resistance in wild-type ABCG2 overexpressing HEK293 cells but not the other two mutant ABCG2 cells. Notably, MK-571 and ONO-1078, known as ABCC1 inhibitors, could restore the sensitivity of BMN-673 in ABCC1-overexpressing cell lines (Figures 5 and 6). Furthermore, Ko143 and cabozantinib, known as ABCG2 inhibitors, could restore the sensitivity of BMN-673 in wild-type ABCG2-overexpressing cell lines (Figures 7 and 8).

As ABCB1 may be a factor of PARP inhibitors resistance in cancer cells, the cytotoxicity of BMN-673 was also tested in transfected ABCB1-overexpressing HEK293 cells. Paclitaxel, a substrate of ABCB1, was used as the positive control, showing decreased cytotoxicity in HEK293/ABCB1 cells compared to the vector control cells. While cisplatin, which is not a substrate of ABCB1, has similar cytotoxicity in these two cell lines. BMN-673 has a similar trend with cisplatin as the cytotoxicity has no difference between ABCB1 overexpressing cells and vector control cells, indicating that ABCB1 overexpression did not cause resistance to BMN-673 (Figure 9).

3.2 Docking analysis of BMN-673 in the drug-binding pocket of ABCC1 and ABCG2

The results showed that BMN-673 docked into the drug-binding site of ABCC1 with an affinity score of -7.8 kcal/mol. Overall, BMN-673 binds in the pocket surrounded

by the transmembrane domains of ABCC1 protein (Figure 10A), partially overlapping the substrate binding site (Figure 10B, 10D). Details of ligand-receptor interaction were displayed in Figure 10B and 10C. The primary factor contributing to the binding affinity of BMN-673 to the ABCC1 protein is hydrophobic interactions. According to Figure 10B, BMN-673 is positioned and stabilized in the hydrophobic cavity formed by Leu381, Phe385, Tyr440, Trp553, Phe594, Ile598, Thr1241, Tyr1242, Asn1244 and Trp1245. Also, BMN-673 was stabilized by hydrogen bonds formed with Trp553, Thr1241, Asn1244, and a pi-pi stacking interaction with Trp1245.

The docking simulation is performed to predict the potential intermolecular interactions between BMN-673 and ABCG2. According to the results, BMN-673 docked into the drug binding site of ABCG2 with a high-affinity score of -10.4 kcal/mol, comparable to known substrate mitoxantrone (-11.4 kcal/mol). Moreover, BMN-673 binds in the pocket partially overlapped with the substrate binding site (Figure 11A, 11D). Details of ligand-receptor interaction were displayed in Figure 11B and 11C. BMN-673 is predicted to be stabilized in the ABCG2 binding pocket majorly via hydrophobic interactions. According to Figure 11B and 11C, BMN-673 is positioned and stabilized in the hydrophobic cavity formed by Phe439, Thr542, Ile543, Val546, Met549 of chain A and Gln398, Val401, Leu405, Phe432, Thr435, Ser440, Val442 of chain B. Also, BMN-673 was stabilized by a hydrogen bond formed with Asn436 of chain B and a pi-pi stacking interaction with Phe439 of chain B.

3.3 BMN-673 inhibited transport function of ABCC1 and ABCG2 by competing with other substrates

As BMN-673 is a potential substrate of ABCC1, the transport of BMN-673 by ABCC1 was investigated by an indirect accumulation and efflux assay using tritium-labeled vincristine. ONO-1078 was used as a positive ABCC1 inhibitor. The result showed that BMN-673 could increase the intracellular accumulation and reduce the efflux of $[^3H]$-vincristine, suggesting a competitive effect with $[^3H]$-vincristine in ABCC1-mediated drug transporting. In addition, $[^3H]$-mitoxantrone was used to evaluate the transport of BMN-673 as BMN-673 is also a potential substrate of ABCG2.

Cabozantinib was used as a positive ABCG2 inhibitor. The result showed that BMN-673 could increase the intracellular accumulation and reduce the efflux of $[^3H]$-mitoxantrone, suggesting a competitive effect with $[^3H]$-mitoxantrone in ABCG2-mediated drug transporting.

3.4 Establishment of the BMN-673-resistant cancer cell line and drug-resistant profile

The BMN-673-resistant ovarian cell line A2780/T4 was eventually developed by selecting the parental A2780 cells in stepwise increasing concentrations of BMN-673 until cells survive in BMN-673 at the concentration up to 4 μM.

The drug-resistant profile of A2780/T4 is summarized in Table 1. The BMN-673 IC$_{50}$ values determined for A2780 cells and A2780/T4 cells were 0.135 μM and 10.712 μM, respectively. A2780/T4 cells exhibited a 79.34-fold resistance to BMN-673 compared to A2780, indicating a resistance-mediated improvement in survival. Besides, A2780/T4 conferred 41.41- and 38.87-fold cross-resistant to typical ABCC1 substrates vincristine and

vinblastine, respectively, which suggested that the human ABCC1 transporter might be a factor mediating the drug resistance in this new cell subline. At the same time, A2780/T4 also conferred 74.43- and 74.80-fold cross-resistant to typical ABCG2 substrates mitoxantrone and topotecan, respectively, which suggested that the human ABCC1 transporter might be a factor mediating the drug resistance in this new cell subline. Only slight cross-resistance (2.77-fold) to doxorubicin, a substrate of both ABCC1 and mutant ABCG2, was exhibited in A2780/T4 cells. However, the IC_{50} values of other ABCB1 or ABCC10 substrates, including paclitaxel and colchicine, were not significantly different between A2780/T4 and its parental cells. Also, A2780/T4 did not show resistance to cisplatin, which is not a substrate of ABCC1 and ABCG2 transporters.

3.5 Resistance to BMN-673 could be reversed by an ABCC1 inhibitor or ABCG2 inhibitor

To verify whether ABCC1 and ABCG2 confer the MDR characteristics in A2780/T4 cells, the reversal effect of the ABCC1 inhibitor, ONO-1078, and ABCG2 inhibitor, cabozantinib, were inspected in A2780 and A2780/T4 cells. The IC_{50} values of ABCC1 substrate vincristine or ABCG2 substrates mitoxantrone in A2780/T4 cells were completely reversed with ONO-1078 or cabozantinib, respectively, to a level comparable to the IC_{50} values in A2780. These suggested that the vincristine resistance was majorly accounted by ABCC1, and ABCG2 majorly mediated the mitoxantrone resistance in A2780/T4 cells. However, only the partial reversal effect of ONO-1078 or cabozantinib was observed in the IC_{50} values of BMN-673 in A2780/T4 cells, which confirmed that both ABCG2 and ABCC1 confer the resistance to BMN-673. Furthermore, the combination

with ONO-1078 or cabozantinib did not affect the IC_{50} of the non-ABC transporters substrate, cisplatin, in both cell lines.

3.6 BMN-673 induced ABCC1 and ABCG2 up-regulation in A2780 cells after 72 h exposure or prolonged selection

To confirm the drug-resistant mechanism of A2780/T4 cells, Western blotting analysis was performed to determine the expression levels of ABCC1 and ABCG2. The significant overexpression of ABCC1 and ABCG2 was observed from the A2780/T4 cells compared to the parental cells after prolonged selection, which is consistent with the previous results. Besides, BMN673 could slightly upregulate the expression of ABCC1 and ABCG2 even after short-term 72 h treatment in both parental and resistant cells.

3.7 BMN-673 induced ABCC1 and ABCG2 up-regulation in A2780 cells after 72 h exposure or prolonged selection

To confirm the drug-resistant mechanism of A2780/T4 cells, Western blotting analysis was performed to determine the expression levels of ABCC1 and ABCG2. The significant overexpression of ABCC1 and ABCG2 was observed from the A2780/T4 cells compared to the parental cells after prolonged selection, which is consistent with the previous results (Figure 15). Besides, BMN673 could slightly upregulate the expression of ABCC1 and ABCG2 even after short-term 72 h treatment in both parental and resistant cells. Figure 16 shows the relative expression level of ABCC1 or ABCG2 from the WB results calculated by ImageJ. The significant overexpression of ABCC1 and ABCG2 was

observed from the A2780/R cells compared to the parental cells, and the upregulation after short-term 72 h treatment has no statistical significance.

3.8 Immunofluorescence analysis indicated the location of ABCC1 and ABCG2 on A2780/T4 membrane

The subcellular localization of ABCC1 and ABCG2 was further determined by immunofluorescence staining. The immunofluorescence images showed a consistent result with that from the western blotting. Here DAPI was used to counter-stain the nuclei. The overexpression of ABCC1 on plasma membranes was revealed in A2780/T4 cells, while the expression of ABCC1 in A2780 cells was not detectable by immunofluorescence under the same staining condition and microscopic settings (Figure 17). Furthermore, the ABCC1 expression could be upregulated in 72h exposure to 0.05 uM of BMN-673. The change of ABCG2 expression by BMN-673 showed the same trend in A2780 and A2780/T4 cells (Figure 18). The ABCG2 expression on the cell membrane was also upregulated by BMN-673 in A2780 and A2780/T4 cells.

3.9 Accumulation of BMN-673 in A2780 and A2780/T4 Cells

Reduced intracellular accumulation of BMN-673 was observed in A2780/T4 cells, which could be reversed by an ABCC1 or ABCG2 inhibitor (Figure 19). The intracellular accumulation of BMN-673 was significantly reduced in A2780/T4 cells compared to the parental cells. Furthermore, when A2780/T4 cells were co-incubated with ONO-1078 or cabozantinib, the intracellular concentration of BMN-673 was significantly increased. Therefore, this result further suggested that functional ABCC1 and ABCG2 overexpression

in A2780/T4 cells significantly contributes to BMN-673 resistance by lowering the intracellular drug level.

3.10 Determination of intracellular drug level of other substrates

To verify whether the overexpressed ABCC1 and ABCG2 in A2780/T4 cells are functional in transporting, and to further confirm that the drug-resistance of A2780/T4 cells was mainly due to an acquired ability to restrict intracellular accumulation by ABCC1 and ABCG2 efflux transporters, the intracellular accumulation of [^{3}H]-vincristine and [^{3}H]-mitoxantrone was measured in A2780 and A2780/T4 cells. Reduced intracellular accumulation and increased efflux of [^{3}H]-vincristine in A2780/T4 cells could be reversed by ABCC1 inhibitor ONO-1078 (Figure 20). A2780/T4 cells exhibited reduced intracellular accumulation of [^{3}H]-vincristine compared to the parental A2780 cells, whereas pre-treatment with 25 μM ONO-1078 elevated [^{3}H]-vincristine accumulation in A2780/T4 cell lines. Inhibition of ABCC1 function by ONO-1078 significantly increased the retention of [^{3}H]-vincristine in A2780/T4, resulting in a similar accumulation level in both cell lines. In addition, reduced intracellular accumulation and increased efflux of [^{3}H]-mitoxantrone was observed in A2780/T4 cells, which could be reversed by ABCG2 inhibitor cabozantinib. [^{3}H]-mitoxantrone was used to confirm that the drug resistance of A2780/T4 cells was mainly due to an acquired ability to restrict intracellular accumulation by the ABCG2 efflux transporter. A2780/T4 cells exhibited reduced intracellular accumulation of [^{3}H]-mitoxantrone compared to the parental A2780 cells, whereas pre-treatment with 5 μM cabozantinib elevated [^{3}H]-mitoxantrone accumulation in A2780/T4 cell lines. Inhibition of ABCG2 function by cabozantinib significantly increased the

retention of [^{3}H]-mitoxantrone in A2780//T4, resulting in a similar accumulation level in both cell lines.

3.11 Knockout of either *ABCC1* or *ABCG2* gene in A2780 and A2780/T4 cell line using CRISPR/Cas9 technique

To confirm the relationship between the overexpression of ABCC1 and ABCG2 with the resistance to BMN-673, the *ABCC1* or *ABCG2* gene knockout sublines of the A2780/T4 cell line was established using a CRISPR/Cas9 technology. The knockout of the *ABCC1* or *ABCG2* gene in A2780/T4 cells was verified by the ABCC1 and ABCG2 protein expression detected using Western blotting (Figure 22). This figure shows that the acquired overexpression of ABCC1 and ABCG2 proteins was confirmed in A2780/T4 cells compared to the parental A2780 cells. The ABCC1 protein level was undetectable in A2780/T4-ABCC1 knockout cells, and the ABCG2 protein level was undetectable in A2780/T4-ABCG2 knockout cells. The gene knockout subline was also developed for the parental A2780 cell line to confirm the ABCC1 and ABCG2 effect in the parental cells.

3.12 The *ABCC1* or *ABCG2* knockout sublines showed reduced resistance to BMN-673 and other ABCC1 or ABCG2 substrate

The MDR phenotype in A2780/T4 cells was significantly reversed by the knockout of the *ABCC1* or *ABCG2* gene. The A2780/T4 knockout cells showed significantly enhanced sensitivity to BMN-673, mitoxantrone, and vincristine compared with A2780/T4 cell lines in Figure 23, confirming the impact of ABCC1 or ABCG2 in the MDR of A2780/T4 cells. In addition, the resistance to BMN-673 was partially reversed by ABCG2

knockout, and the resistance can be further lessened by ABCC1 inhibitor MK-571 or ONO-1078. Similarly, the resistance to BMN-673 was partially reversed by ABCC1 knockout, and the resistance can be further lessened by ABCG2 inhibitor Ko143 or cabozantinib.

This indicated that the resistance to BMN-673 in A2780/T4 cells is mediated by the combined effect of ABCC1 and ABCG2 overexpression. To confirm this, specific ABCC1 substrate vincristine and ABCG2 substrate mitoxantrone were tested in these knockout cells. The previous reversal experiment showed that in the A2780/T4 cells, the mitoxantrone resistance is majorly contributed by ABCG2 but not ABCC1. In contrast, vincristine resistance is majorly contributed by ABCC1 but not ABCG2. The results from the knockout cells verified this finding. As shown in Figure 23, mitoxantrone resistance was completely reversed by inhibitor or *ABCG2* knockout. In contrast, *ABCC1* knockout did not affect the IC_{50} of mitoxantrone. This figure also confirmed the successful knockout of *ABCG2* because ABCG2 inhibitors could not affect mitoxantrone IC_{50} after *ABCG2* knockout. Moreover, Figure 23 shows that vincristine resistance was completely reversed by ABCC1 inhibitor or *ABCC1* knockout and was not affected by *ABCG2* knockout. Again, it confirmed the successful knockout of *ABCC1* because ABCC1 inhibitors could not affect vincristine IC_{50} after *ABCC1* knockout.

By contrast, for cisplatin, which is not an ABCC1 and ABCG2 substrate, the IC_{50} values were consistent among the cell lines regardless of the knockout of *ABCC1* or *ABCG2* genes or the presence of the inhibitors.

3.13 Establishment of the tumor xenograft mice model using A2780/T4 cell line

To further verify whether the *in vitro* findings could extend to an *in vivo* model, A2780 cells and A2780/T4 cells were implanted subcutaneously into athymic female nude mice to establish tumor xenograft mice models. The tumor size and body weight have been recorded. After the animal study, the tumors were also used to extract the BMN-673 for HPLC analysis to verify the drug accumulation in the *in vivo* model.

3.14 The *in vitro* findings could be translated into *in vivo* evaluation with the same BMN-673 resistant pattern

As demonstrated in the results, BMN-673 at 0.3 mg/kg with or without cabozantinib or ONO-1078 showed different degrees of anti-cancer activity in tumor xenograft mice without apparent adverse effects or weight loss (Figure 28). The images of resected tumors (Figure 24 and 25) at the end of the treatment show the anti-cancer effect of BMN-673 with or without cabozantinib or ONO-1078 on A2780 and A2780/T4 tumors in female nude mice. The inhibitory effect of BMN-673 in A2780 tumors was much more significant than that in the A2780/T4 tumors, suggesting a BMN-673 resistant phenotype in A2780/T4 xenograft model. Similarly, the implanted A2780/T4 tumors were significantly diminished in the combination treatment group compared to the vehicle and BMN-673 alone.

From the data of tumor volumes in Figure 26, BMN-673 alone at 0.3 mg/kg dose demonstrated significant growth retardation in the drug-sensitive A2780 tumors but not in the drug-resistance A2780/T4 tumors. Furthermore, the tumor volume of implanted

A2780/T4 cells was significantly diminished in the combination treatment group compared to the vehicle and BMN-673 alone.

The intratumoral level of BMN-673 shown in Figure 27 decreased by 75% in drug-resistant A2780/T4 tumors compared to the parental tumors, suggesting the *in vivo* drug accumulation pattern is consistent with the *in vitro* study. In addition, the combinational treatment elevated the BMN-673 level in A2780/T4 tumors by about 2-fold.
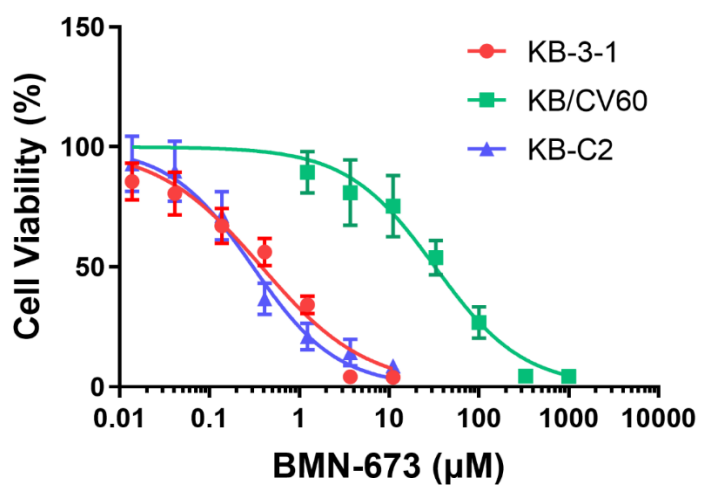
Figure 3. The concentration-survival curves of BMN-673 on drug-selected ABCB1- and ABCC1-overexpressing cell lines (KB-C2 and KB/CV60) and their parental cell line (KB-3-1).

Each dot is displayed as mean ± SD from three experiments performed independently.
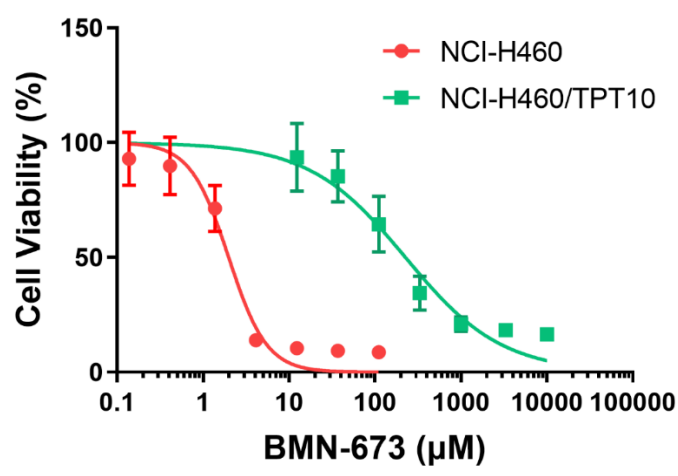
Figure 4. The concentration-survival curves of BMN-673 on drug-selected ABCG2-overexpressing cell lines (NCI-H460/TPT10) and its parental cell line (NCI-H460). Each dot is displayed as mean ± SD from three experiments performed independently.
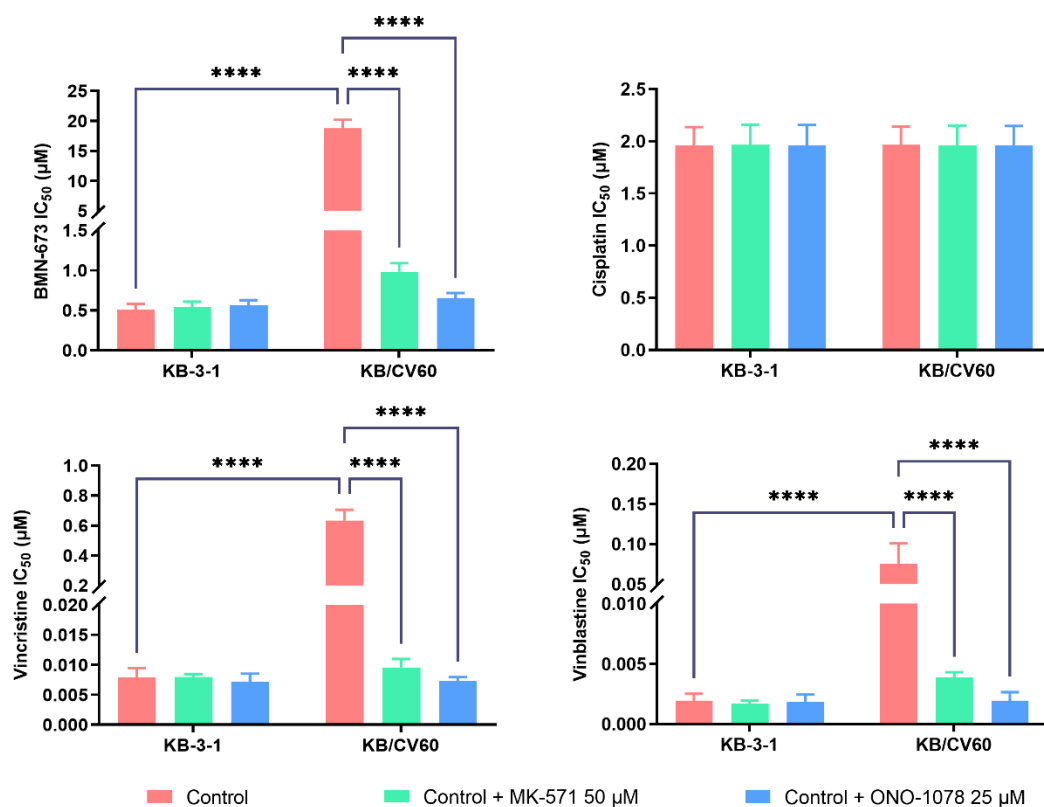
Figure 5. Effect of MK-571 and ONO-1078 on the IC_{50} values of BMN-673, cisplatin, vincristine, and vinblastine in KB-3-1 and KB/CV60 cells.

Columns and error bars represented mean ± SD of IC_{50} values acquired from three independent experiments in triplicate. ****$p < 0.001$.
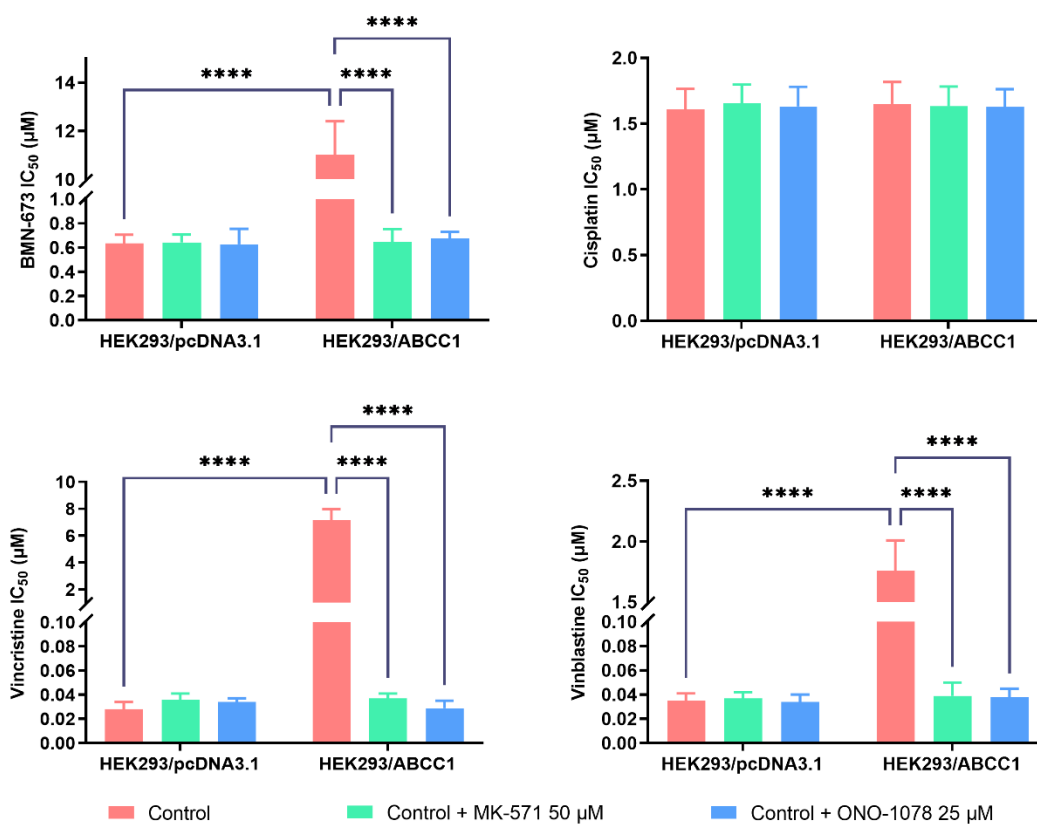
Figure 6. Effect of MK-571 and ONO-1078 on the IC_{50} values of BMN-673, cisplatin, vincristine, and vinblastine in HEK293/pcDNA3.1 and HEK293/ABCC1 cells.

Columns and error bars represented mean ± SD of IC_{50} values acquired from three independent experiments in triplicate. ****$p < 0.001$.
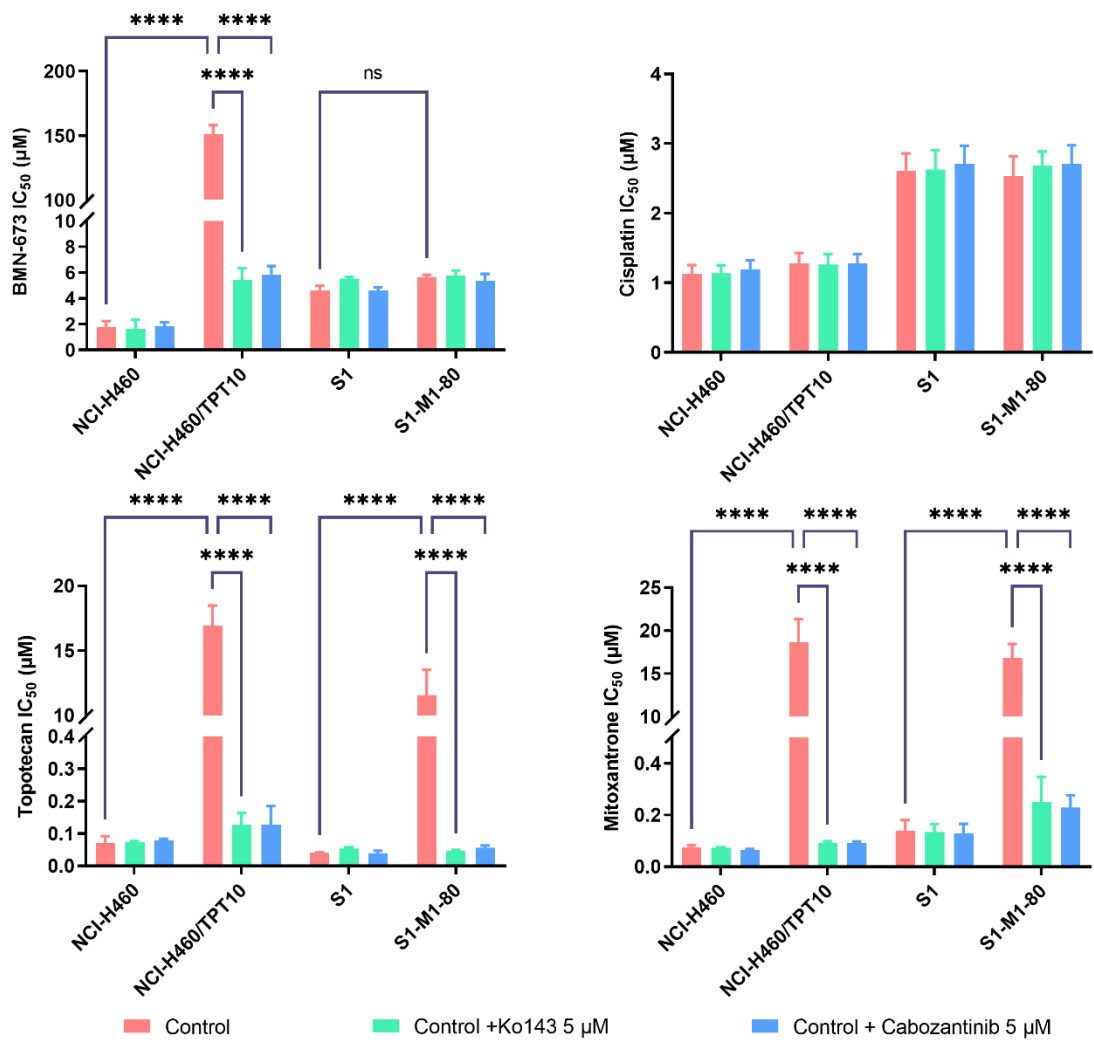
Figure 7. Effect of Ko143 and Cabozantinib on the IC_{50} values of BMN-673, cisplatin, topotecan, and mitoxantrone in NCI-H460 and NCI-H460/TPT10 cells, and S1 and S1-M1-80 cells.

Columns and error bars represented mean $\pm$ SD of IC_{50} values acquired from three independent experiments in triplicate. ****$p < 0.001$.
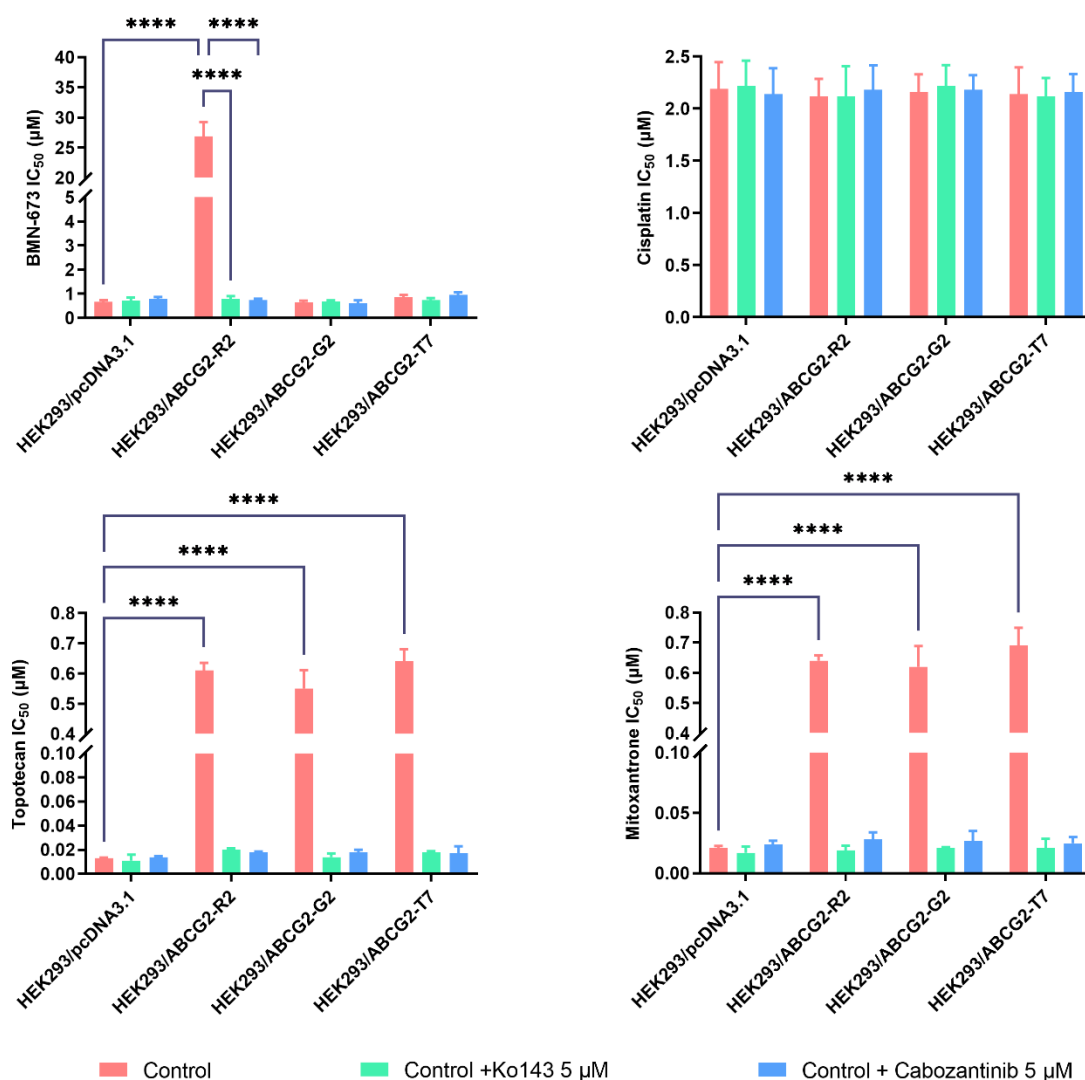
Figure 8. Effect of Ko143 and cabozantinib on the IC$_{50}$ values of BMN-673, cisplatin, topotecan, and mitoxantrone in HEK293/pcDNA3.1, HEK293/ABCG2-R2, HEK293/ABCG2-G2, and HEK293/ABCG1-T7 cells.

Columns and error bars represented mean ± SD of IC$_{50}$ values acquired from three independent experiments in triplicate. ****p < 0.001.
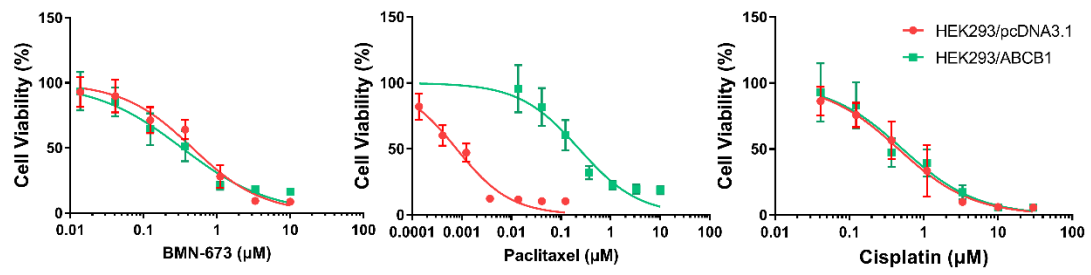
Figure 9. The concentration-survival curves of BMN-673 on transfected ABCB1-overexpressing HEK293/ABCB1 cell line and its vector control cell line HEK293/pcDNA3.1.

Each dot is displayed as mean ± SD from three experiments performed independently.
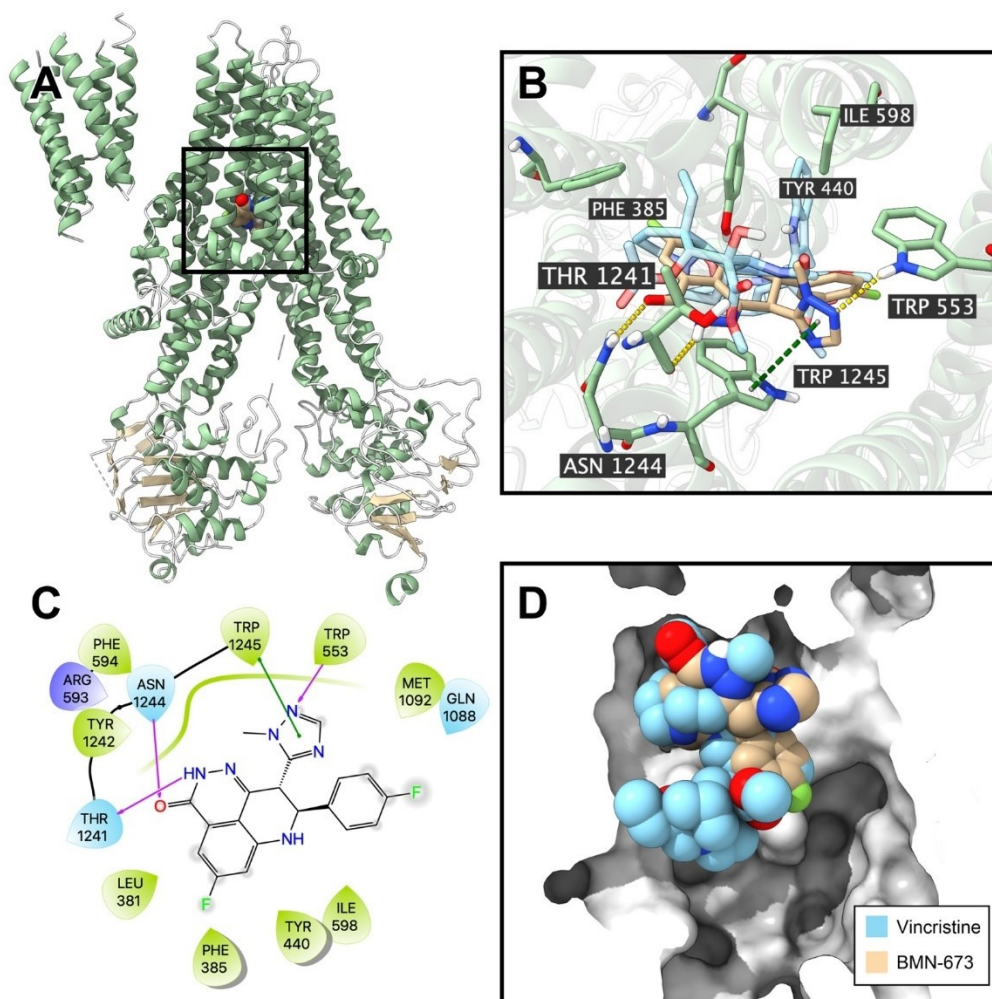
Figure 10. Interaction between BMN-673 and ABCC1.

A) Overview of the best-scoring pose of BMN-673 in the drug binding pocket of ABCC1 protein (5UJA). ABCC1 was displayed as colored ribbons (helix: green; strand: yellow; coil: white). BMN-673 was displayed as colored balls. Carbon: yellow; nitrogen: blue; oxygen: red; fluoride: lime. B) Details of interactions between BMN-673/vincristine and ABCC1 binding pocket. ABCC1 helices were displayed as colored ribbons. Critical residues were displayed as colored sticks (carbon: green (BMN-673) or light blue (vincristine); oxygen: red; nitrogen: blue; hydrogen: white; fluoride: lime). Hydrogen bonds were displayed as yellow dashed lines. Pi-pi stacking was displayed as green dash lines. C) 2D diagram of the interaction between BMN-673 and ABCC1. Amino acids within 3 Å from BMN-673 were displayed as colored bubbles (green: hydrophobic; blue: polar). Purple solid lines with arrow indicate hydrogen bonds. Green solid line indicates pi-pi stacking interaction. D) Binding poses of BMN-673 and ABCC1 substrate vincristine in ABCC1 binding pocket.
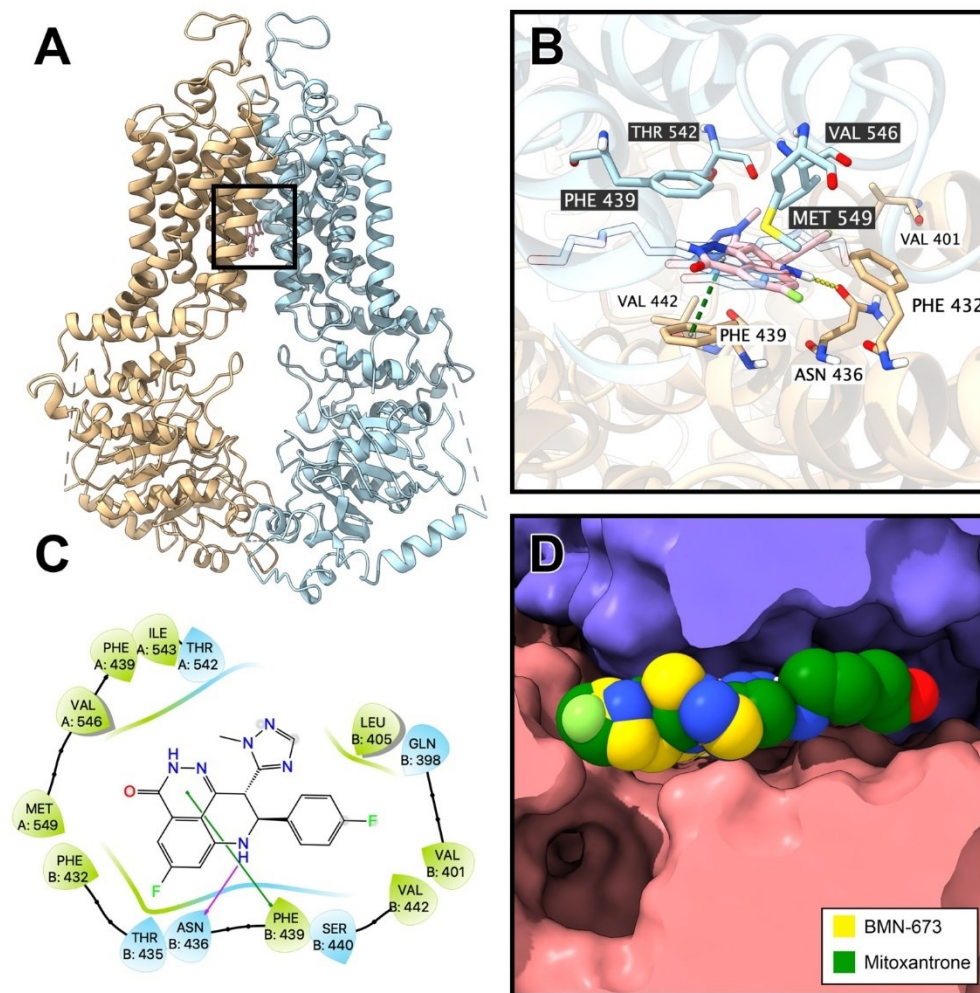
Figure 11. Interaction between BMN-673 and ABCG2.

A) Overview of the best-scoring pose of BMN-673 in the drug binding pocket of ABCG2 protein (6VXI). ABCG2 was displayed as colored ribbons (chain A: blue; chain B: yellow). BMN-673 was displayed as colored sticks. Carbon: light pink; nitrogen: blue; oxygen: red; fluoride: lime. B) Details of interactions between BMN-673/mitoxantrone and ABCG2 binding pocket. ABCG2 helices were displayed as colored ribbons. Important residues were displayed as colored sticks (carbon: light pink (BMN-673) or blue (mitoxantrone); oxygen: red; nitrogen: blue; hydrogen: white; fluoride: lime). Hydrogen bonds were displayed as yellow dashed lines. Pi-pi stacking was displayed as green dash lines. C) 2D diagram of the interaction between BMN-673 and ABCG2. Amino acids within 3 Å from BMN-673 were displayed as colored bubbles (green: hydrophobic; blue: polar). Purple solid lines with arrow indicate hydrogen bonds. Green solid line indicates pi-pi stacking interactions. D) Binding poses of BMN-673 and ABCG2 substrate mitoxantrone in ABCG2 binding pocket.
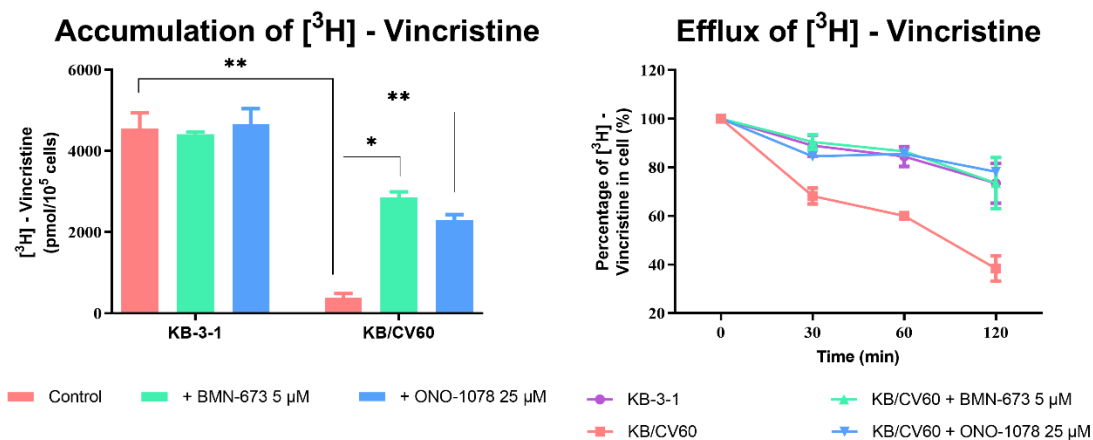
Figure 12. The tritium-labeled mitoxantrone accumulation in ABCC1 overexpressing KB/CV60 and its corresponding drug-sensitive cells KB-3-1.

ONO-1078 functioned as a known inhibitor for ABCC1. **$p < 0.01$, *$p < 0.05$
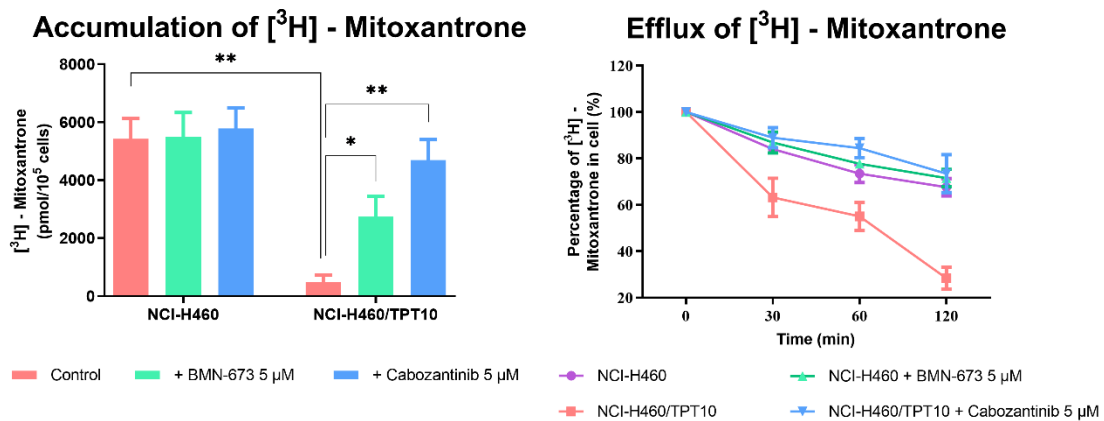
Figure 13. The tritium-labeled mitoxantrone accumulation in ABCG2-overexpressing NCI-H460/TPT10 cells and its corresponding drug-sensitive cells NCI-H460. Cabozantinib functioned as a known inhibitor for ABCG2. $**p < 0.01$, $*p < 0.05$
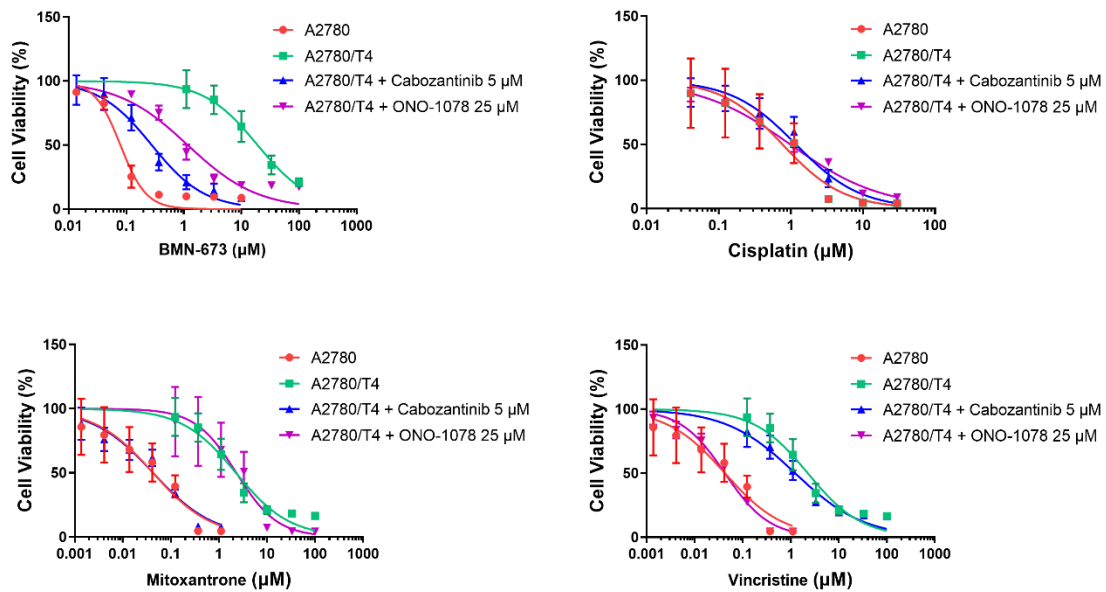
Figure 14. Cytotoxic activity of BMN-673, cisplatin, mitoxantrone, and vincristine in A2780 and A2780/T4 cells.

The concentration-response curves for the drugs with or without verified ABCC1 inhibitor ONO-1078 or ABCG2 inhibitor cabozantinib. Each dot is expressed as mean ± SD from a representative of three independent experiments.
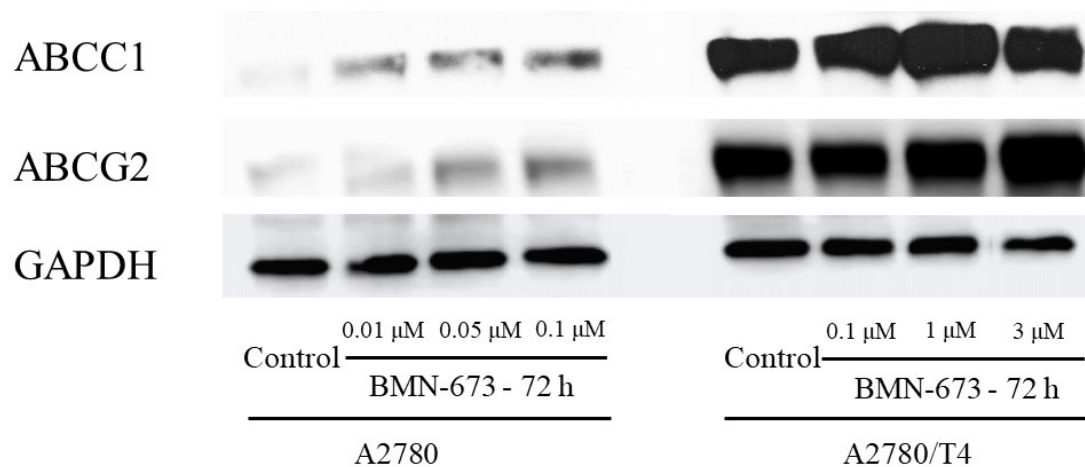
Figure 15. Protein expression profile of A2780/T4 and parental A2780 cells. Western blot analysis detect ABCC1 and ABCG2 expression in A2780/T4 cell lines. The adopted loading control was GAPDH.
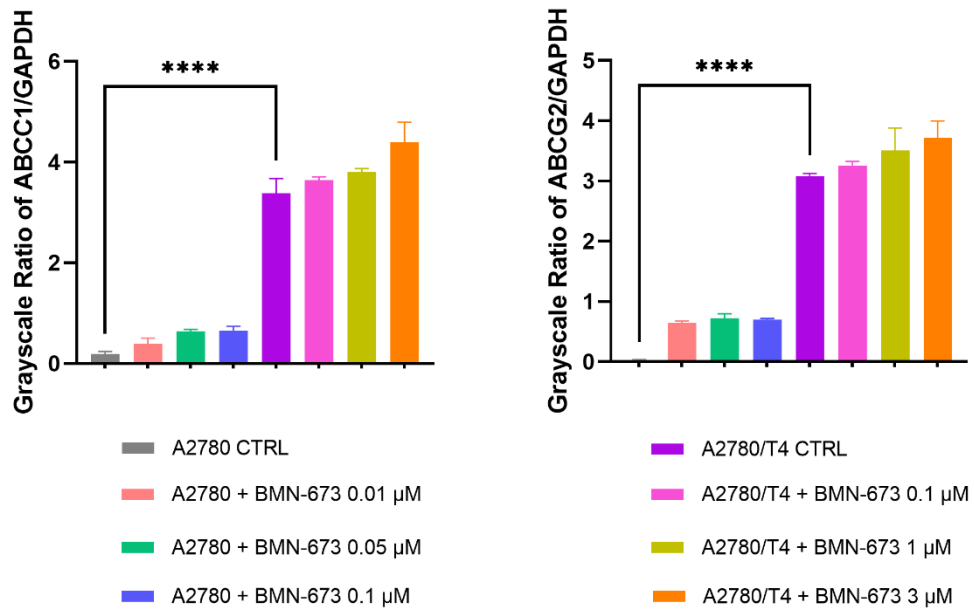
Figure 16. The relative protein expression was calculated based on the ratio of the target protein versus the loading control protein GAPDH.

Columns and error bars represented average values with SD from three independent measurements. ****p < 0.001, comparing the resistant cell line to the parental cell line.
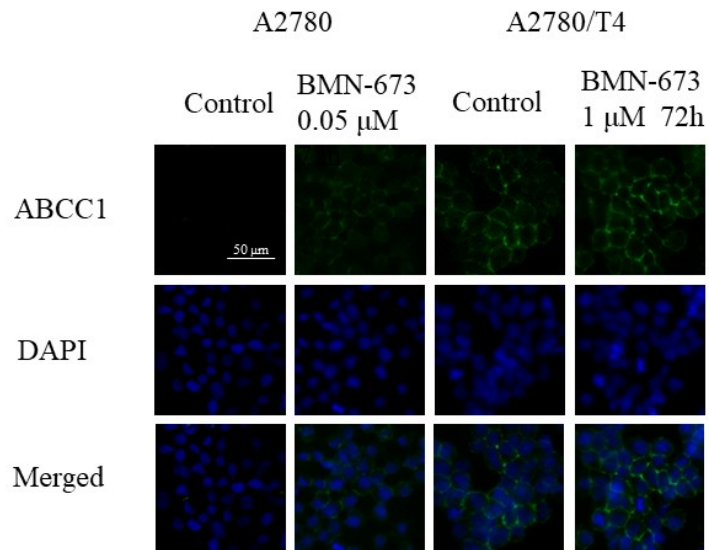
Figure 17. Immunofluorescence microscopic images of A2780 and A2780/T4 cells. ABCC1 and DAPI fluorescence micrographs were combined to create a merged image. ABCC1 expression was shown by green fluorescence; cell nuclei were stained blue by DAPI. This experiment has been done with triplicate wells in replicated independent tests.
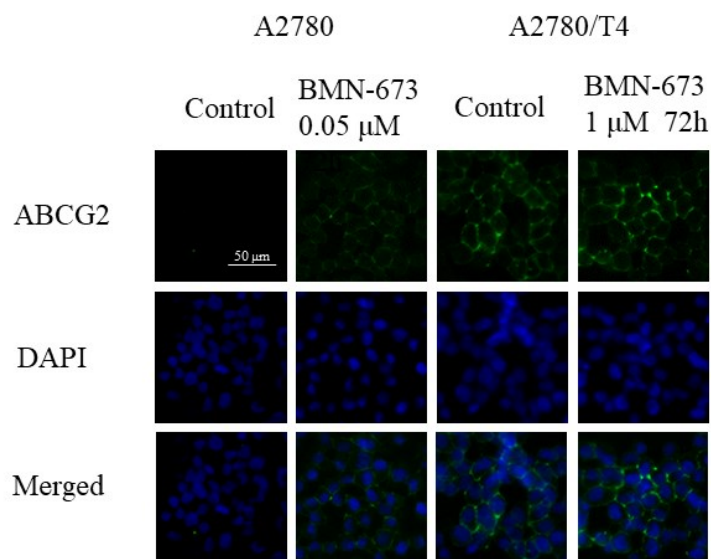
Figure 18. Immunofluorescence microscopic images of A2780 and A2780/T4 cells. ABCG2 and DAPI fluorescence micrographs were combined to create a merged image. ABCG2 expression was shown by green fluorescence; cell nuclei were stained blue by DAPI. This experiment has been done with triplicate wells in replicated independent tests.
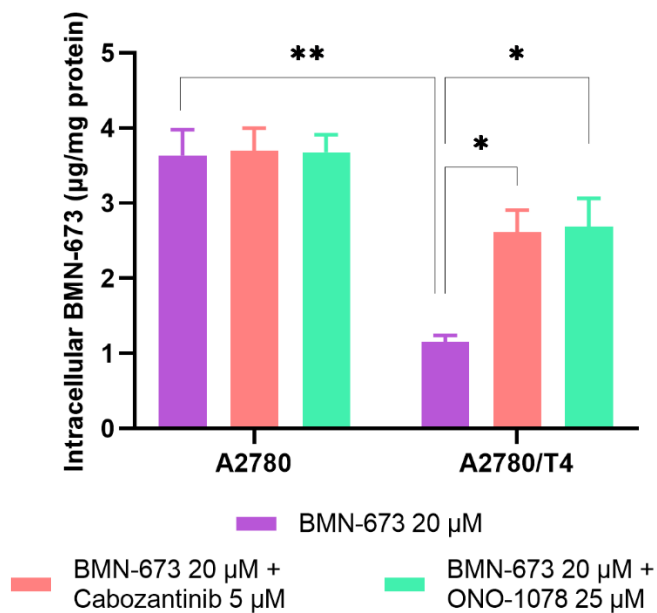
Figure 19. BMN-673 accumulation in A2780 and A2780/T4 cells was detected by HPLC technology.

The detection of intracellular accumulation of BMN-673 in cells after 2 h exposure to 20 μM BMN-673 with or without 2 h pretreatment with 25 μM ONO-1078 or 5 μM cabozantinib. Columns and error bars represented average values with SD from three independent measurements. **p < 0.01, *p < 0.05
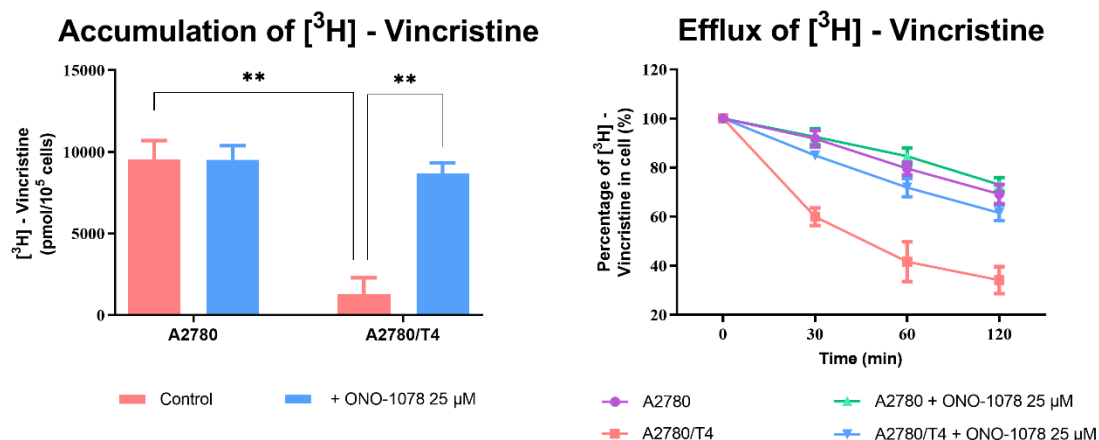
Figure 20. The cellular accumulation and efflux activity of [³H]-vincristine in A2780 and A2780/T4 cells.

ONO-1078 was used as a positive control of ABCC1 inhibition. Columns and error bars represented average values with SD from three independent measurements. Data points with error bars represented the mean ± SD of three independent experiments in triplicate. **$p < 0.01$
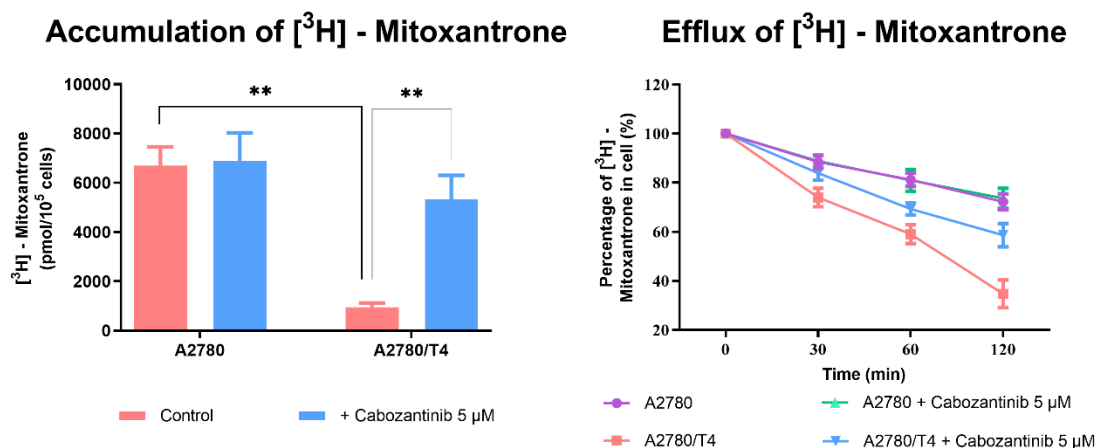
Figure 21. The cellular accumulation and efflux activity of [^{3}H]-mitoxantrone in A2780 and A2780/T4 cells.

Cabozantinib was used as a positive control of ABCG2 inhibition. Columns and error bars represented average values with SD from three independent measurements. Data points with error bars represented the mean ± SD of three independent experiments in triplicate. **$p < 0.01$
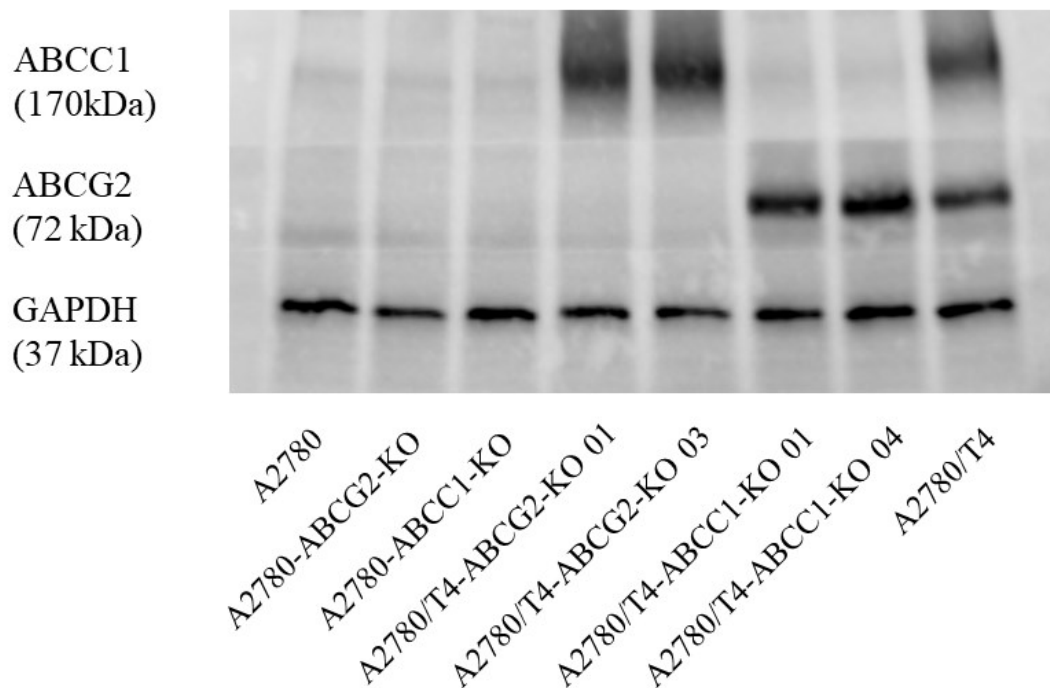
Figure 22. Verification of A2780/T4-ABCC1 knockout and A2780/T4-ABCG2 knockout (ko) subline.

Western blot on the expression levels of ABCC1 and ABCG2 in A2780, A2780/T4, and different colonies obtained from A2780 or A2780/T4 cells transfected with the CRISPR plasmid targeting ABCC1 or ABCG2 gene. GAPDH was used as a loading control.
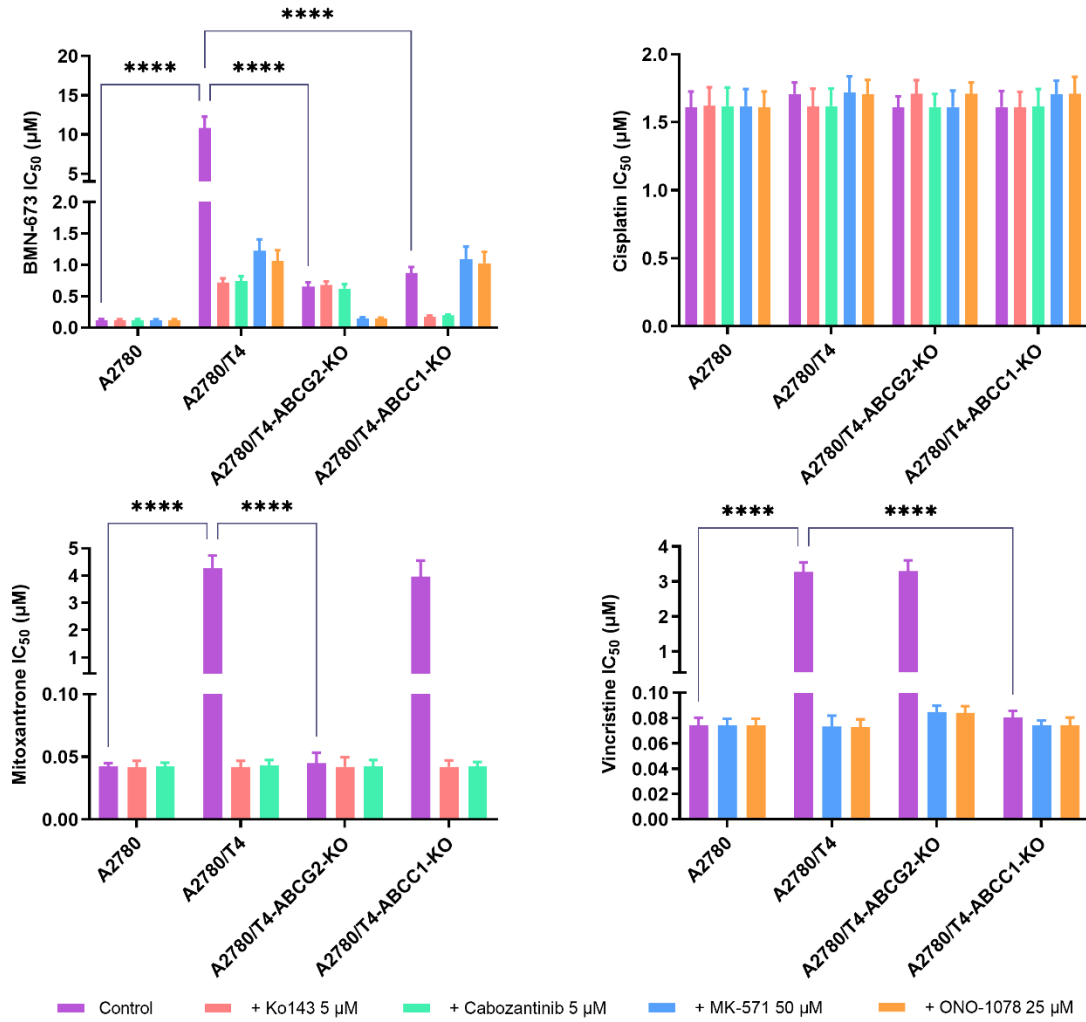
Figure 23. Abolishment of drug resistance ABCC1 or ABCG2 gene knockout in A2780/T4 Cells.

Cell viability was determined by MTT assay and displayed the changes in response to different concentrations of BMN-673, cisplatin, mitoxantrone, and vincristine in drug-resistant A2780/T4 and the parental A2780 cells, with or without ABCC1 or ABCG2 inhibitor, and in A2780/T4-ABCC1 or A2780/T4- ABCG2 knockout (ko) cells. Columns with error bars represented the mean $IC_{50} \pm SD$ of at least three independent experiments, each done in triplicate. Statistical analysis was performed to compare the IC_{50} values. ****$p < 0.001$
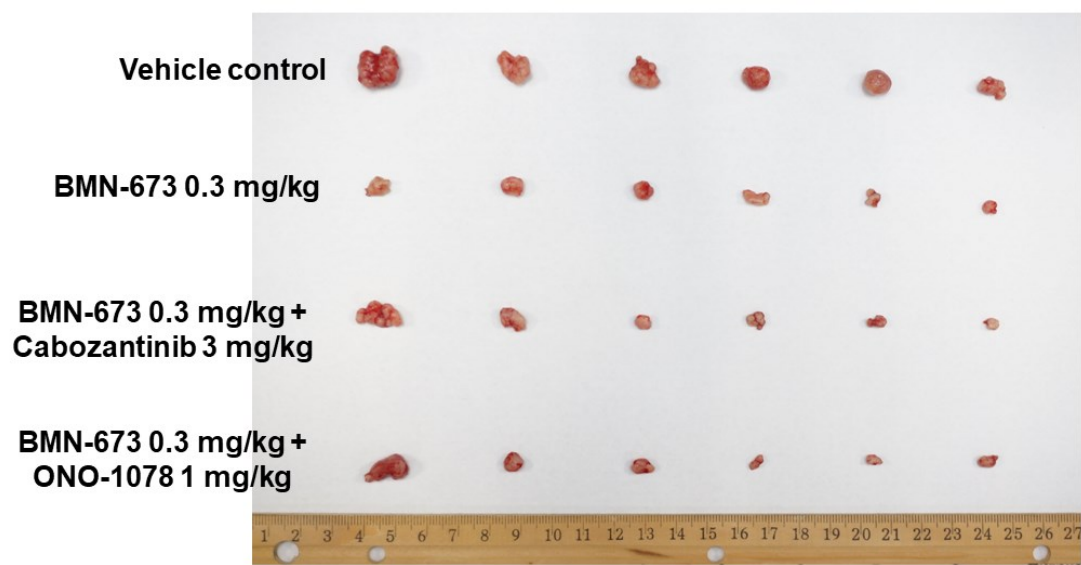
Figure 24. Effect of BMN-673 and the combination with cabozantinib or ONO-1078 on the growth of A2780 tumors in female nude mice.

The images of resected tumors from nude mice (n = 6 per treatment group) implanted with A2780 tumors at the end of the treatment period.
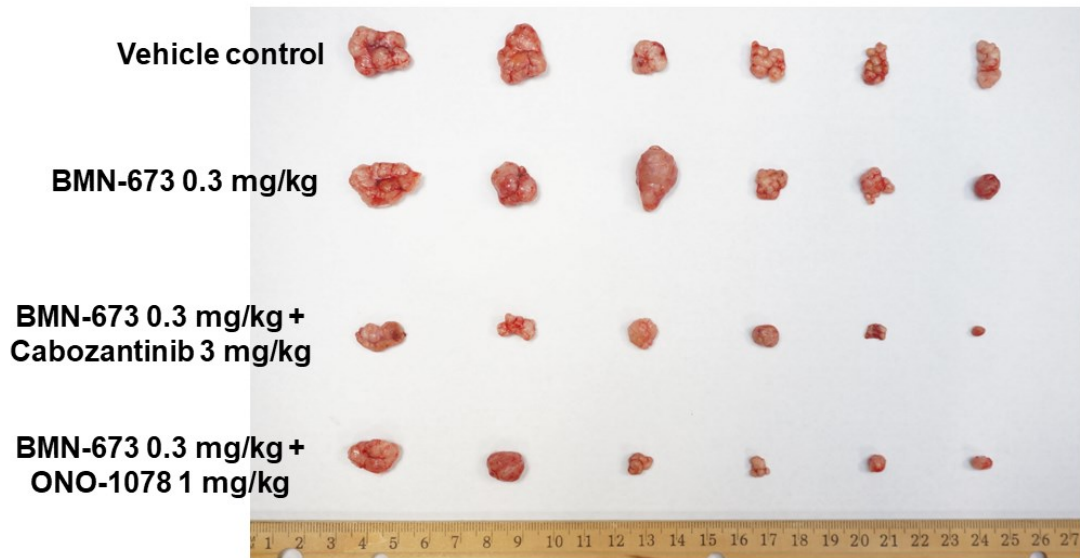
Figure 25. Effect of BMN-673 and the combination with cabozantinib or ONO-1078 on the growth of A2780/T4 tumors in female nude mice.

The images of resected tumors from nude mice (n = 6 per treatment group) implanted with A2780/T4 tumors at the end of the treatment period.
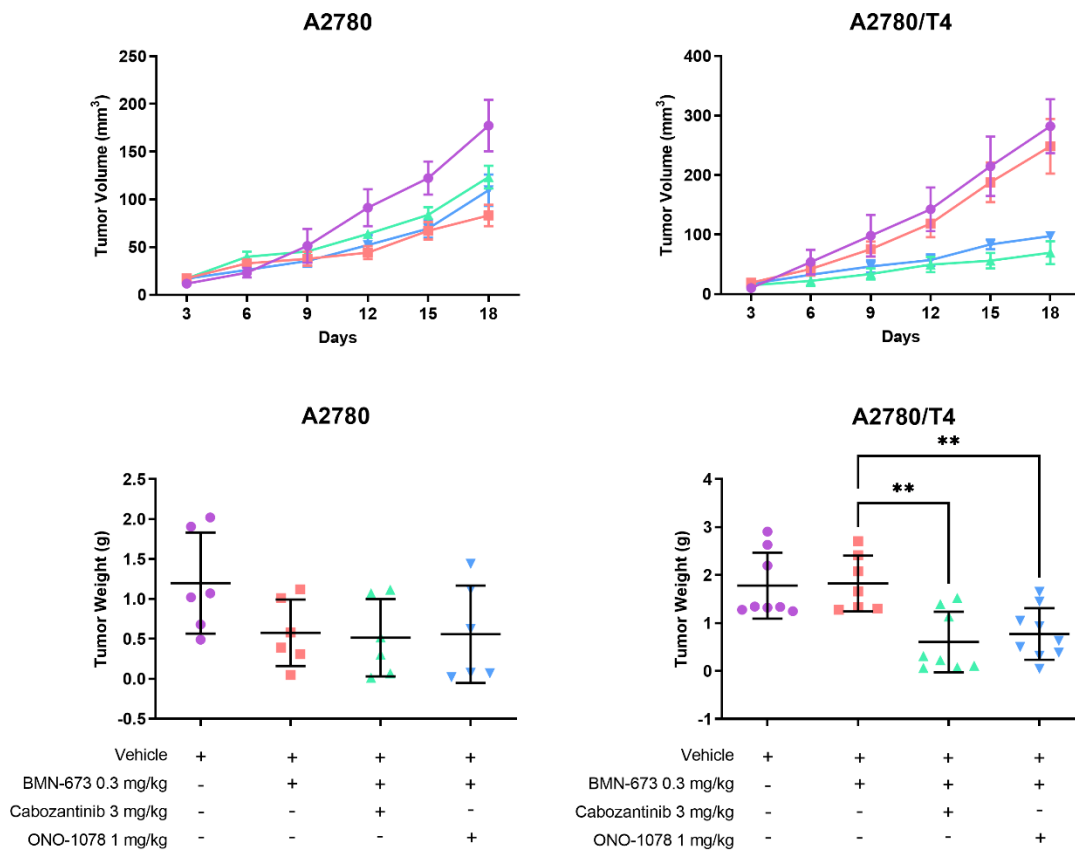
Figure 26. The changes in A2780 and A2780/T4 tumor weight after the implantation and changes in A2780 and A2780/T4 tumor volume throughout the study.

Data points and error bars represent the mean and SD of tumor volume (n = 6). Scatter points represented the weights of the excised A2780 and A2780/T4 tumors at the end of the 18-day treatment period (n = 6 per treatment group). Lines and error bars represented the mean weight values and SD. **p < 0.01
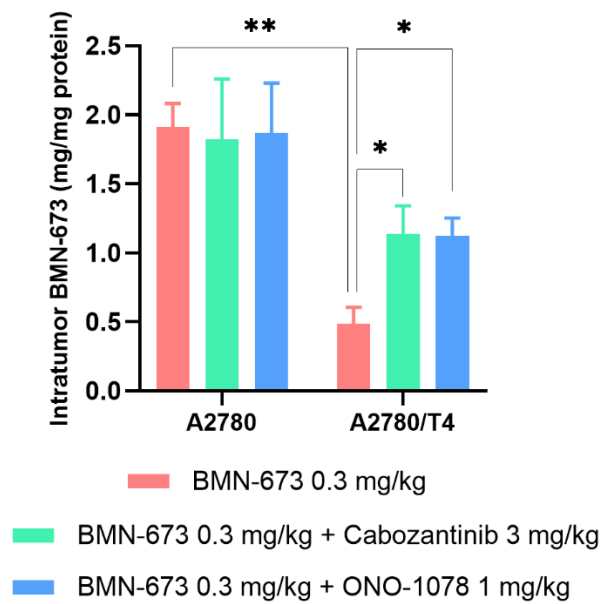
Figure 27. Intratumor BMN-673 concentrations in A2780 and A2780/T4 tumors after 18-day following administration of BMN-673 alone or the combination.

Data are expressed as mean ± SD from three independent experiments (n = 3). **p < 0.01, *p < 0.05
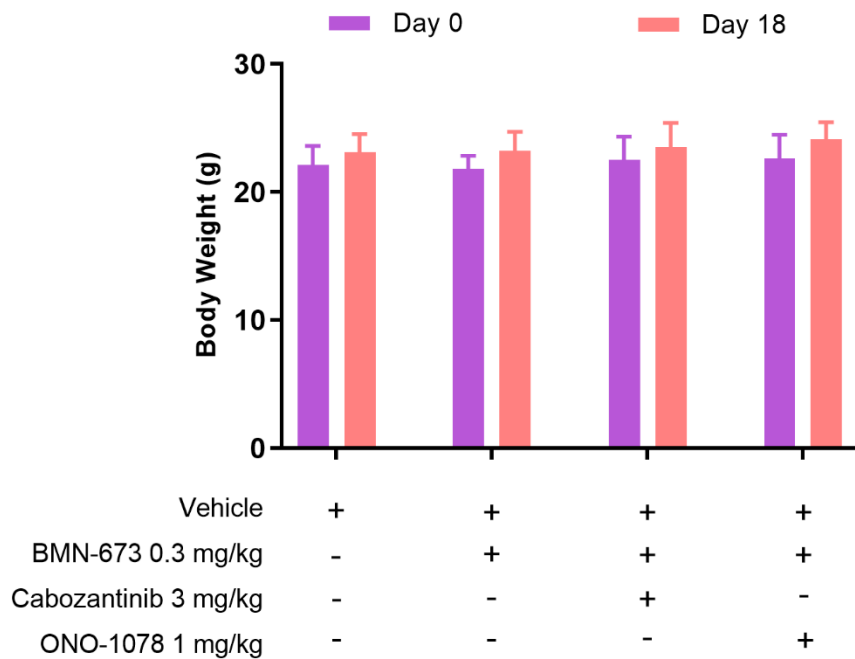
Figure 28. Body weight changes during the treatment period.
Columns and error bars represent the mean and SD of body weight change represented by the percentage of body weight at day 0 (n = 6).

Table 1. The drug-resistance profile of A2780/T4 cell line

| Anticancer drugs | $IC_{50} \pm SD$ (μM) | | Resistant Fold (RF) |
	A2780	A2780/T4	
BMN-673	0.135 ± 0.017	10.712 ± 0.953 *	79.34
mitoxantrone	0.061 ± 0.007	4.540 ± 0.375 *	74.43
topotecan	0.116 ± 0.036	8.677 ± 0.914 *	74.80
vincristine	0.073 ± 0.005	3.023 ± 0.215 *	41.41
vinblastine	0.194 ± 0.017	7.541 ± 0.178 *	38.87
doxorubicin	1.834 ± 0.179	5.083 ± 0.571	2.77
paclitaxel	2.519 ± 0.194	2.822 ± 0.036	1.12
colchicine	28.185 ± 1.619	30.835 ± 2.597	1.10
cisplatin	1.648 ± 0.156	1.808 ± 0.106	1.11

IC_{50}, 50% inhibition concentration. RF: resistant-fold represents IC_{50} value for different anticancer drugs of A2780/T4 cells divided by IC_{50} value for different anticancer drugs of A2780 cells. *Indicates a significant difference between IC_{50} value of A2780 and that of A2780/T4 (*$p < 0.05$) by Student's t-test.

CHAPTER 4
DISCUSSION

The study of PARP inhibitors has led to critical new insights into the mechanisms of PARP inhibitor resistance. Each PARP inhibitor has a different chemical structure and multiple off-target effects [114]. This suggests that novel PARP inhibitors may have a therapeutic effect in drug-resistant tumors [102]. Among the resistance mechanisms identified to date, restoration of homology-directed DNA repair is frequently observed *in vitro* and *in vivo* [100]. Resistance to PARP inhibitors also needs to be further explored. The most common acquired resistance mechanism to PARP inhibitors involves secondary mutations that restore BRCA1/2 protein function [83, 90]. Combining PARP inhibitors with drugs that inhibit HR may effectively sensitize ovarian cancer with spontaneous or acquired HR to PARP inhibitors in clinical therapeutic strategies [85, 100]. The discovery and characterization of BMN-673 as a potent, selective, orally bioavailable inhibitor of PARP1/2 provides an essential addition to the field of PARP inhibitors [85]. Its efficacy in PARP capture is early evidence that BMN-673 may improve clinical outcomes in BRCA-mutant malignancies [85, 90]. In MDR-exhibiting cancer, cells that acquire resistance to one drug often develop resistance to a range of other structurally and functionally unrelated anticancer agents, resulting in cancer recurrence and even relapse or death [105]. Thus, identifying the underlying mechanisms of drug resistance is critical for developing new treatment strategies to overcome MDR and improve chemotherapeutic efficacy.

The experiments with cell viability assay in drug-selected and gene-transfected cell lines indicated that BMN-673 had high potency with IC_{50} values at the nanomolar level. Furthermore, ABCC1 or ABCG2 overexpression could confer resistance to BMN-673 in cancer cells. Importantly, BMN-673 resistance was only observed in wild-type ABCG2-

overexpressing drug-induced cancer cell lines and transfected HEK293 cell lines. It is known that switching arginine to glycine (R > G) or threonine (R > T) at amino-acid 482 in the *ABCG2* gene may occur due to drug-induced mutation or genetic polymorphisms, which could cause substrate specificity and different resistance levels to substrate-drugs [115-117]. Mitoxantrone is found to be a substrate drug of all ABCG2 variations; however, doxorubicin and daunorubicin are transported by only mutant R482T or R482G but not by the wild-type R482 ABCG2 [115, 118]. Also, compared with wild-type ABCG2, an R482G mutation confers relatively less resistance to topotecan [118], and novobiocin, a known ABCG2 inhibitor, affects the wild-type ABCG2 completely but only reverse mutant ABCG2 partially [35]. The results showed that ABCG2 variation at position 482 affected BMN-673 resistance. No difference in the BMN-673 IC_{50} between the mutant ABCG2 overexpressing cells with the parental cells, while the significant resistant fold of BMN-673 was observed between the wild-type ABCG2 overexpressing cells with the parental cells. Thus, only wild-type ABCG2 but not mutant ABCG2 (R482G or R482T) may confer resistance to BMN-673 among ABCG2 transporters. Together, we hypothesized that the efficacy of BMN-673 could be compromised in the presence of ABCC1 and wild-type ABCG2. Also, BMN-673-induced resistance could be sensitized by an ABCC1 or ABCG2 reference inhibitor, suggesting that ABCC1- or ABCG2-overexpression is the mechanism of BMN-673 resistance.

Based on the cytotoxicity assay results, the in silico molecular docking was conducted to explore the interaction of BMN-673 with ABCC1 or ABCG2. The molecular docking was performed using atomic structures of vincristine-bound ABCC1 (PDB ID: 5UJA) and mitoxantrone-bound ABCG2 (PDB ID: 6VXI). The docking results showed

that BMN-673 shares similar binding sites with known substrates for ABCC1 or ABCG2, which suggested that BMN-673 interacts with the drug-binding pocket of ABCC1 or ABCG2 and behaves as a substrate for ABCC1 or ABCG2 transporter. It is documented that some substrates of ABC transporters [119, 120], such as lapatinib, imatinib, nilotinib, and dasatinib, can compete with another drug substrate for transport function [121]; as a result, a repurposed drug substrate can sensitize MDR-associated ABC transporters to another drug substrate by the competition. Tritium-labeled substrate accumulation and efflux assays were performed to investigate the effect of BMN-673 on transport function conferred by ABCC1 or ABCG2. In competition with ABCC1 substrate vincristine or ABCG2 substrate mitoxantrone, the results indicated that BMN-673 could increase substrate-drug accumulation in the MDR cell lines but not in their corresponding parental cell lines. This effect might result from a high concentration of BMN-673 competitively inhibiting the efflux of vincristine or mitoxantrone while impeding the transport function of ABCC1 or ABCG2, respectively, and in turn, increasing intracellular substrate accumulation. The accumulation study was carried out with a short-term treatment (4 h), which protected cells from the influence of the change in cell viability and other cellular functions, while the concentrations of BMN-673 used for these experiments were higher than the IC$_{50}$ value. The results further confirmed that BMN-673 competitively inhibits the efflux of other ABCC1 or ABCG2 substrates, which may affect the pharmacokinetic profile of other ABCC1 or ABCG2 substrate-drugs. However, these findings do not warrant further testing of BMN-673 as a reversal agent.

In order to garner a broader understanding of the mechanisms of BMN-673 resistance in ovarian cancer, a BMN-673-resistant ovarian cell line by maintaining the

parental A2780 cells in stepwise increasing concentration of BMN-673 and termed this drug-resistant subline as A2780/T4. The established cell line was first tested to confirm its resistance to BMN-673, and the drug-resistant profile was characterized. After a 6-month selection with BMN-673 and 2-months of culturing without BMN-673, A2780/T4 cells conferred a 79.34-fold resistance against BMN-673 compared to parental A2780 cells, confirming the acquisition of BMN-673 resistance in the newly established cell line. ABCB1, ABCC1, and ABCG2 are the three major ABC transporters present in MDR cancer cells, and each of them has a broad substrate range overlapping with the other two. Cross-resistance to ABCC1 substrates vincristine and vinblastine, ABCG2 substrates mitoxantrone and topotecan were observed as reduced cytotoxicity in A2780/T4 cell line compared to its parental cell line, which suggested a potential involvement of ABCC1 and ABCG2 in MDR of A2780/T4 cells. A2780/T4 cells displayed no resistance to non-ABCC1 and -ABCG2 substrates such as paclitaxel, colchicine, and cisplatin, suggesting that ABCB1 or ABCC10 may not involve in the MDR induced by BMN-673. The no difference in the doxorubicin IC_{50} values between parental and the new resistant cell lines might verify that BMN-673 is only susceptible to wild-type ABCG2-mediated MDR but not the mutant ABCG2 [122].

After that, immunoblotting analysis was performed to evaluate protein expression after BMN-673 treatment. The Western blotting results and immunofluorescence imaging results confirmed that the high expression of ABCC1 and ABCG2 were majorly distributed on the plasma membrane of the drug-resistant cells A2780/T4, leading to a hypothesis that the overexpression of ABCC1 and ABCG2 transporter on cell membrane functions to pump out the intracellular anticancer drugs thereby resulting in drug resistance in

A2780/T4 cells. This hypothesis was further verified by accessing the reversal effect of a potent ABCC1 inhibitor, ONO-1078, or ABCG2 inhibitor, cabozantinib, respectively, and the abolishment of drug resistance by *ABCC1* or *ABCG2* gene knockout in A2780/T4 cells. Pre-treatment with ONO-1078 or cabozantinib at a non-toxic concentration significantly re-sensitized A2780/T4 cells to BMN-673 and other ABCC1 or ABCG2 substrate drugs, respectively, with IC_{50} values comparable to those in the drug-sensitive A2780 cells. Additionally, the remarkably diminished BMN-673 accumulation in A2780/T4 cells could be restored by inhibiting ABCC1 using ONO-1078 or inhibiting ABCG2 using cabozantinib, which indicated that the drug resistance of A2780/T4 could be entirely reversed by inhibiting the drug efflux function of ABCC1 or ABCG2 function. Meanwhile, the IC_{50} values of a non-ABCC1 and -ABCG2 substrate, cisplatin, remained relatively constant between parental and resistant cells with or without the inhibitors, indicating that the inhibitors may reduce BMN-673 resistance in A2780/T4 cells by the ABCC1 or ABCG2 inhibitory mechanism showed in other ABCC1 or ABCG2 overexpressing MDR models.

Besides functional inhibition of ABCC1 or ABCG2, loss of ABCC1 or ABCG2 protein expression by gene knockout also abolished the MDR feature of A2780/T4 cells. Furthermore, the ABCC1 inhibitor ONO-1078 could not sensitize A2780/T4-ABCC1 knockout cells to BMN-673 as it did on ABCC1 overexpressing A2780/T4 cells. At the same time, it could completely reverse the BMN-673 resistance in A2780/T4-ABCG2 knockout cells, and the ABCG2 inhibitor cabozantinib could not sensitize A2780/T4-ABCG2 knockout cells to BMN-673 as it did on ABCG2 overexpressing A2780/T4 cells. In contrast, it could completely reverse the BMN-673 resistance in A2780/T4-ABCC1

knockout cells, which confirms the involvement of both ABCC1 and ABCG2 in the resistance to BMN-673. These findings validate that the elevated protein expression of ABCC1 and ABCG2 are both the leading cause of drug resistance in A2780/T4 cells. Therefore, the main mechanism responsible for BMN-673 resistance in A2780/T4 cells is more likely to be the active removal of BMN-673 from the cells via both the overexpression of ABCC1 and wild-type ABCG2 on the cell membrane.

Although *in vitro* models have been valuable in studying cancer MDR and developing novel anticancer drugs, their direct relevance to clinical cancer cases has been uncertain. Cultured cancer cells that have adapted to the *in vitro* micro-environment are often differ from the actual tumor found in patients because they do not capture the regulations from the extracellular matrix, cell-matrix interactions, cell-cell interactions in a three-dimensional tumor structure, and the multi-cellular heterogeneous components of the tumor micro-environment such as stromal cells and blood vessels [123]. The xenograft animal models based on conventional cancer cell lines have been developed and used for decades to improve the shortage. In order to assess the applicability of the A2780/T4 cell line to test MDR reversal agents *in vitro* and to verify whether the *in vitro* resistance characteristic can be retained in the *in vivo* settings, a tumor xenograft nude mouse model implanted with A2780 and A2780/T4 tumors in the left and right flank near the armpit, respectively, was further established and investigated. In consideration of the clinical relevance of the *in vivo* study, the designed dose of BMN-673 [124, 125], ABCC1 inhibitor ONO-1078 [126, 127], and ABCG2 inhibitor cabozantinib [123] was evaluated from previous *in vivo* studies.

The results of the animal studies indicated that the A2780/T4 xenograft model presented the same drug-resistance phenotype to BMN-673 as the *in vitro* studies. This resistance could be reversed by the ABCC1 inhibitor ONO-1078 or ABCG2 inhibitor cabozantinib in the xenograft mouse model. As demonstrated in Figure 28, BMN-673 at 0.3 mg/kg with or without 3 mg/kg of cabozantinib or 1 mg/kg of ONO-1078 showed different degrees of anti-cancer activity in tumor xenograft mice without apparent adverse effects or weight loss. BMN-673 alone at 0.3 mg/kg dose demonstrated significant growth retardation in the drug-sensitive A2780 tumors (Figures 24) but not in the drug-resistance A2780/T4 tumors (Figures 25). Similarly, the inhibitory effect of BMN-673 on tumor weight was significantly lower in the A2780/T4 tumors than in the A2780 tumors (Figure 26), suggesting a BMN-673 resistant phenotype in A2780/T4 xenograft model. The average tumor volume and weight of implanted A2780 cells and A2780/T4 cells were significantly diminished in the combination treatment group compared to the vehicle and BMN-673 alone groups (Figures 24 and 25).

The *in vivo* study showed lower BMN-673 efficacy in A2780/T4 tumors than in A2780 tumors. Potential anticancer effects from both the combination treatment groups were observed, which verified the findings of BMN-673 resistant phenotype of A2780/T4 cell line and the reversal capability of ONO-1078 or cabozantinib in A2780/T4 cells could be extended to *in vivo* xenograft models. The A2780 cell line and its drug-resistant sublines may serve as sound models for cancer pharmacology research as they are likely to possess clinically relevant characteristics, such as drug resistance *in vitro* and in *vivo*. The results also supported that the A2780/T4 cell line could be a favorable model for studying BMN-673 resistance, ABCC1- and ABCG2-mediated MDR, and pharmacological evaluations on

potential MDR reversal agents. In an *in vivo* setting, it is more likely that multiple factors are involved in cancer MDR than in a monolayer cell culture with general growth media. Tumor cells can influence the surrounding micro-environment by releasing extracellular signals, promoting tumor vascular proliferation, and inhibiting peripheral immune cells, and all these factors can affect the growth and resistance phenotype of tumor cells [128, 129]. Intra-tumor heterogenicity in the implanted tumors and tumor-host interactions, such as the interplay between the tumors and their micro-environment [130], may also contribute to the ABCC1- and ABCG2-mediated MDR observed in A2780/T4 xenograft models.

CHAPTER 5
SUMMARY

Cancer is one of the leading causes of death in decades. Although chemotherapy has been verified to inhibit tumor growth in clinical application in safe concentrations, MDR frequently develops during chemotherapy treatment, which sharply reduces the therapeutic efficacy. The overexpression of ABC transporters, which reduces intracellular drug concentration, is the primary factor in the development of MDR. This work focused on the relationship of ABCC1 and ABCG2 to the drug resistance of the PARP inhibitor BMN-673. The overexpression of ABCC1 or ABCG2 conferred resistance to BMN-673, and this effect can be antagonized by known ABCC1 or ABCG2 inhibitors. The newly established A2780/T4 cell line helps study ABCC1- and ABCG2-mediated MDR and other PARP-inhibitor-related resistance mechanisms in ovarian cancer. The data in this study suggested that the elevated expression of ABCC1 and ABCG2 on the plasma membrane of A2780/T4 cells are the major factor accounting for its MDR phenotype. Still, much remains to be further verified and elucidated regarding the interactions of BMN-673 with ABCC1 or ABCG2 transporter at the molecular level and the other possible MDR mechanisms in the BMN-673-induced resistance model. The established models in this study can be helpful for the in-depth investigation of these interactions, which will be crucial for future drug design. The reversal effect of ONO-1078 or cabozantinib against ABCC1- or ABCG2-mediated BMN-673 resistance has been confirmed in the BMN-673-resistant human ovarian A2780/T4 tumor xenograft model. The established A2780/T4 cell line and its xenograft model could serve as an invaluable, clinical-relevant resource for future drug screening and developing novel PARP inhibitor approaches to eradicate MDR in ovarian cancer.

In conclusion, I report for the first time that the potent PARP inhibitor BMN-673 might affect by ABCC1- and ABCG2-mediated MDR in ovarian cancer. The clinical therapeutic effect of BMN-673 needs to be monitored during the treatment period. Further studies are also warranted to confirm whether the ABCC1 or ABCG2 inhibitors could be contributed to improving clinical outcomes in patients receiving BMN-673. Collectively, this project presents *in vitro* and *in vivo* evidence that BMN-673 is susceptible to ABCC1- and ABCG2-mediated drug resistance and provides important indications for follow-up clinical use of BMN-673.

REFERENCES

1.   Torre, L.A., et al., *Global cancer statistics, 2012.* CA Cancer J Clin, 2015. **65**(2): p. 87-108.

2.   Siegel, R.L., et al., *Cancer statistics, 2022.* CA: A Cancer Journal for Clinicians, 2022. **72**(1): p. 7-33.

3.   Siegel, R.L., K.D. Miller, and A. Jemal, *Cancer statistics, 2018.* CA Cancer J Clin, 2018. **68**(1): p. 7-30.

4.   Miller, K.D., et al., *Cancer treatment and survivorship statistics, 2022.* CA: A Cancer Journal for Clinicians, 2022. **72**(5): p. 409-436.

5.   Holohan, C., et al., *Cancer drug resistance: an evolving paradigm.* Nature Reviews Cancer, 2013. **13**: p. 714.

6.   Wang, J.Q., et al., *ATP-binding cassette (ABC) transporters in cancer: A review of recent updates.* J Evid Based Med, 2021. **14**(3): p. 232-256.

7.   Horsey, A.J., et al., *The multidrug transporter ABCG2: still more questions than answers.* Biochem Soc Trans, 2016. **44**(3): p. 824-30.

8.   Kathawala, R.J., et al., *The modulation of ABC transporter-mediated multidrug resistance in cancer: A review of the past decade.* Drug Resistance Updates, 2015. **18**: p. 1-17.

9.   Chun, S.-Y., et al., *Lapatinib enhances the cytotoxic effects of doxorubicin in MCF-7 tumorspheres by inhibiting the drug efflux function of ABC transporters.* Biomedicine & Pharmacotherapy, 2015. **72**: p. 37-43.

10.   Giacomini, K.M., et al., *Membrane transporters in drug development.* Nat Rev Drug Discov, 2010. **9**(3): p. 215-36.

11. Filomeni, G., et al., *6-(7-Nitro-2,1,3-benzoxadiazol-4-ylthio)hexanol, a specific glutathione S-transferase inhibitor, overcomes the multidrug resistance (MDR)-associated protein 1–mediated MDR in small cell lung cancer.* Molecular Cancer Therapeutics, 2008. **7**(2): p. 371-379.

12. Rodriguez-Antona, C. and M. Ingelman-Sundberg, *Cytochrome P450 pharmacogenetics and cancer.* Oncogene, 2006. **25**: p. 1679.

13. Shoemaker, R.H., *Genetic and Epigenetic Factors in Anticancer Drug Resistance.* JNCI: Journal of the National Cancer Institute, 2000. **92**(1): p. 4-5.

14. Li, H. and B.B. Yang, *Friend or foe: the role of microRNA in chemotherapy resistance.* Acta Pharmacologica Sinica, 2013. **34**: p. 870.

15. Wilson, C.S., et al., *DNA Topoisomerase IIα in Multiple Myeloma: A Marker of Cell Proliferation and Not Drug Resistance.* Modern Pathology, 2001. **14**: p. 886.

16. Bedi, A., et al., *BCR-ABL-mediated inhibition of apoptosis with delay of G2/M transition after DNA damage: a mechanism of resistance to multiple anticancer agents.* Blood, 1995. **86**(3): p. 1148-58.

17. Camidge, D.R., W. Pao, and L.V. Sequist, *Acquired resistance to TKIs in solid tumours: learning from lung cancer.* Nature Reviews Clinical Oncology, 2014. **11**: p. 473.

18. Milane, L., Z. Duan, and M. Amiji, *Role of hypoxia and glycolysis in the development of multi-drug resistance in human tumor cells and the establishment of an orthotopic multi-drug resistant tumor model in nude mice using hypoxic pre-conditioning.* Cancer Cell International, 2011. **11**(1): p. 3.

19. Dean, M., T. Fojo, and S. Bates, *Tumour stem cells and drug resistance.* Nature Reviews Cancer, 2005. **5**: p. 275.

20. Li, Y.J., et al., *Autophagy and multidrug resistance in cancer.* Chin J Cancer, 2017. **36**(1): p. 52.

21. Kumar, P., et al., *Autophagy and transporter-based multi-drug resistance.* Cells, 2012. **1**(3): p. 558-75.

22. Gottesman, M.M., T. Fojo, and S.E. Bates, *Multidrug resistance in cancer: role of ATP-dependent transporters.* Nat Rev Cancer, 2002. **2**(1): p. 48-58.

23. Thomas, H. and H.M. Coley, *Overcoming multidrug resistance in cancer: an update on the clinical strategy of inhibiting p-glycoprotein.* Cancer Control, 2003. **10**(2): p. 159-65.

24. Bissett, D., et al., *Phase I and pharmacokinetic study of D-verapamil and doxorubicin.* Br J Cancer, 1991. **64**(6): p. 1168-71.

25. Kozovska, Z., V. Gabrisova, and L. Kucerova, *Colon cancer: Cancer stem cells markers, drug resistance and treatment.* Biomedicine & Pharmacotherapy, 2014. **68**(8): p. 911-916.

26. Seok, L.J., et al., *Reduced drug accumulation and multidrug resistance in human breast cancer cells without associated P-glycoprotein or MRP overexpression.* Journal of Cellular Biochemistry, 1997. **65**(4): p. 513-526.

27. Kusuhara, H. and Y. Sugiyama, *ATP-binding cassette, subfamily G (ABCG family).* Pflügers Archiv - European Journal of Physiology, 2007. **453**(5): p. 735-744.

28. Gujarati, N.A., et al., *Design, synthesis and biological evaluation of benzamide and phenyltetrazole derivatives with amide and urea linkers as BCRP inhibitors.* Bioorganic & Medicinal Chemistry Letters, 2017. **27**(20): p. 4698-4704.

29. Zhang, J.T., *Biochemistry and pharmacology of the human multidrug resistance gene product, ABCG2.* Zhong Nan Da Xue Xue Bao Yi Xue Ban, 2007. **32**(4): p. 531-41.

30. Kawabata, S., et al., *Expression and functional analyses of breast cancer resistance protein in lung cancer.* Clin Cancer Res, 2003. **9**(8): p. 3052-7.

31. Wiese, M., *BCRP/ABCG2 inhibitors: a patent review (2009-present).* Expert Opin Ther Pat, 2015. **25**(11): p. 1229-37.

32. Rabindran, S.K., et al., *Reversal of a novel multidrug resistance mechanism in human colon carcinoma cells by fumitremorgin C.* Cancer Res, 1998. **58**(24): p. 5850-8.

33. Rabindran, S.K., et al., *Fumitremorgin C reverses multidrug resistance in cells transfected with the breast cancer resistance protein.* Cancer Res, 2000. **60**(1): p. 47-50.

34. Sugimoto, Y., et al., *Reversal of breast cancer resistance protein-mediated drug resistance by estrogen antagonists and agonists.* Mol Cancer Ther, 2003. **2**(1): p. 105-12.

35. Ken, S., et al., *Reversal of breast cancer resistance protein (BCRP/ABCG2)-mediated drug resistance by novobiocin, a coumermycin antibiotic.* International Journal of Cancer, 2004. **108**(1): p. 146-151.

36.   Zhang, G.N., et al., *Modulating the function of ATP-binding cassette subfamily G member 2 (ABCG2) with inhibitor cabozantinib.* Pharmacol Res, 2017. **119**: p. 89-98.

37.   Lei, Z.N., et al., *Cabozantinib Reverses Topotecan Resistance in Human Non-Small Cell Lung Cancer NCI-H460/TPT10 Cell Line and Tumor Xenograft Model.* Front Cell Dev Biol, 2021. **9**: p. 640957.

38.   Cai, B., et al., *Nuclear Multidrug-Resistance Related Protein 1 Contributes to Multidrug-Resistance of Mucoepidermoid Carcinoma Mainly via Regulating Multidrug-Resistance Protein 1: A Human Mucoepidermoid Carcinoma Cells Model and Spearman's Rank Correlation Analysis.* PLoS ONE, 2013. **8**(8): p. e69611.

39.   Leslie, E.M., R.G. Deeley, and S.P. Cole, *Multidrug resistance proteins: role of P-glycoprotein, MRP1, MRP2, and BCRP (ABCG2) in tissue defense.* Toxicol Appl Pharmacol, 2005. **204**(3): p. 216-37.

40.   Wang, J.Q., et al., *Multidrug resistance proteins (MRPs): Structure, function and the overcoming of cancer multidrug resistance.* Drug Resist Updat, 2021. **54**: p. 100743.

41.   Slot, A.J., S.V. Molinski, and S.P. Cole, *Mammalian multidrug-resistance proteins (MRPs).* Essays Biochem, 2011. **50**(1): p. 179-207.

42.   He, S.M., et al., *Structural and functional properties of human multidrug resistance protein 1 (MRP1/ABCC1).* Curr Med Chem, 2011. **18**(3): p. 439-81.

43.   Mao, Q., R.G. Deeley, and S.P. Cole, *Functional reconstitution of substrate transport by purified multidrug resistance protein MRP1 (ABCC1) in phospholipid vesicles.* J Biol Chem, 2000. **275**(44): p. 34166-72.

44.   Sugiyama, T. and Y. Sadzuka, *Theanine and glutamate transporter inhibitors enhance the antitumor efficacy of chemotherapeutic agents.* Biochimica et Biophysica Acta (BBA) - Reviews on Cancer, 2003. **1653**(2): p. 47-59.

45.   Huang, Y. and W. Sadee, *Membrane transporters and channels in chemoresistance and -sensitivity of tumor cells.* Cancer Lett, 2006. **239**(2): p. 168-82.

46.   Cole, S.P., et al., *Overexpression of a transporter gene in a multidrug-resistant human lung cancer cell line.* Science, 1992. **258**(5088): p. 1650-4.

47.   He, X., et al., *Alternative splicing of the multidrug resistance protein 1/ATP binding cassette transporter subfamily gene in ovarian cancer creates functional splice variants and is associated with increased expression of the splicing factors PTB and SRp20.* Clin Cancer Res, 2004. **10**(14): p. 4652-60.

48.   Kunická, T. and P. Souček, *Importance of ABCC1 for cancer therapy and prognosis.* Drug Metabolism Reviews, 2014. **46**(3): p. 325-342.

49.   Bai, P. and C. Cantó, *The role of PARP-1 and PARP-2 enzymes in metabolic regulation and disease.* Cell Metab, 2012. **16**(3): p. 290-5.

50.   Gibson, B.A. and W.L. Kraus, *New insights into the molecular and cellular functions of poly(ADP-ribose) and PARPs.* Nat Rev Mol Cell Biol, 2012. **13**(7): p. 411-24.

51.   Valabrega, G., et al., *Differences in PARP Inhibitors for the Treatment of Ovarian Cancer: Mechanisms of Action, Pharmacology, Safety, and Efficacy.* Int J Mol Sci, 2021. **22**(8).

52.   Krishnakumar, R. and W.L. Kraus, *The PARP side of the nucleus: molecular actions, physiological outcomes, and clinical targets.* Mol Cell, 2010. **39**(1): p. 8-24.

53.   Chaitanya, G.V., A.J. Steven, and P.P. Babu, *PARP-1 cleavage fragments: signatures of cell-death proteases in neurodegeneration.* Cell Commun Signal, 2010. **8**: p. 31.

54.   Boussios, S., et al., *Poly (ADP-Ribose) Polymerase Inhibitors: Talazoparib in Ovarian Cancer and Beyond.* Drugs R D, 2020. **20**(2): p. 55-73.

55.   Flanagan, K.L., et al., *Sex and Gender Differences in the Outcomes of Vaccination over the Life Course.* Annu Rev Cell Dev Biol, 2017. **33**: p. 577-599.

56.   Chiu, L.Y., et al., *Oxidative stress initiates DNA damager MNNG-induced poly(ADP-ribose)polymerase-1-dependent parthanatos cell death.* Biochem Pharmacol, 2011. **81**(3): p. 459-70.

57.   !!! INVALID CITATION !!! [81].

58.   Moore, K.N., et al., *Niraparib monotherapy for late-line treatment of ovarian cancer (QUADRA): a multicentre, open-label, single-arm, phase 2 trial.* Lancet Oncol, 2019. **20**(5): p. 636-648.

59.   Pazzaglia, S. and C. Pioli, *Multifaceted Role of PARP-1 in DNA Repair and Inflammation: Pathological and Therapeutic Implications in Cancer and Non-Cancer Diseases.* Cells, 2019. **9**(1).

60. Morales, J., et al., *Review of poly (ADP-ribose) polymerase (PARP) mechanisms of action and rationale for targeting in cancer and other diseases.* Crit Rev Eukaryot Gene Expr, 2014. **24**(1): p. 15-28.

61. Prasad, R., et al., *Mammalian Base Excision Repair: Functional Partnership between PARP-1 and APE1 in AP-Site Repair.* PLoS One, 2015. **10**(5): p. e0124269.

62. Sriram, C.S., et al., *Alternative mechanisms of inhibiting activity of poly (ADP-ribose) polymerase-1.* Front Biosci (Schol Ed), 2016. **8**(1): p. 123-8.

63. Metzger, M.J., B.L. Stoddard, and R.J. Monnat, Jr., *PARP-mediated repair, homologous recombination, and back-up non-homologous end joining-like repair of single-strand nicks.* DNA Repair (Amst), 2013. **12**(7): p. 529-34.

64. Rahman, S., et al., *A Survey of Reported Disease-Related Mutations in the MRE11-RAD50-NBS1 Complex.* Cells, 2020. **9**(7).

65. Wang, Q., et al., *Rad17 recruits the MRE11-RAD50-NBS1 complex to regulate the cellular response to DNA double-strand breaks.* Embo j, 2014. **33**(8): p. 862-77.

66. Gupte, R., Z. Liu, and W.L. Kraus, *PARPs and ADP-ribosylation: recent advances linking molecular functions to biological outcomes.* Genes Dev, 2017. **31**(2): p. 101-126.

67. Farmer, H., et al., *Targeting the DNA repair defect in BRCA mutant cells as a therapeutic strategy.* Nature, 2005. **434**(7035): p. 917-21.

68. Hartwell, L.H., et al., *Integrating genetic approaches into the discovery of anticancer drugs.* Science, 1997. **278**(5340): p. 1064-8.

69. Alhmoud, J.F., et al., *DNA Damage/Repair Management in Cancers.* Cancers (Basel), 2020. **12**(4).

70.   Jones, P., et al., *Niraparib: A Poly(ADP-ribose) Polymerase (PARP) Inhibitor for the Treatment of Tumors with Defective Homologous Recombination.* J Med Chem, 2015. **58**(8): p. 3302-14.

71.   Bryant, H.E., et al., *Specific killing of BRCA2-deficient tumours with inhibitors of poly(ADP-ribose) polymerase.* Nature, 2005. **434**(7035): p. 913-7.

72.   Fong, P.C., et al., *Inhibition of poly(ADP-ribose) polymerase in tumors from BRCA mutation carriers.* N Engl J Med, 2009. **361**(2): p. 123-34.

73.   Pal, T., et al., *BRCA1 and BRCA2 mutations account for a large proportion of ovarian carcinoma cases.* Cancer, 2005. **104**(12): p. 2807-16.

74.   Huang, X., et al., *Leveraging an NQO1 Bioactivatable Drug for Tumor-Selective Use of Poly(ADP-ribose) Polymerase Inhibitors.* Cancer Cell, 2016. **30**(6): p. 940-952.

75.   *Erratum for the Perspective: "Laying a trap to kill cancer cells: PARP inhibitors and their mechanisms of action" by Y. Pommier, M. J. O'Connor, J. de Bono.* Sci Transl Med, 2016. **8**(368): p. 368er7.

76.   Lord, C.J. and A. Ashworth, *PARP inhibitors: Synthetic lethality in the clinic.* Science, 2017. **355**(6330): p. 1152-1158.

77.   Wu, L., et al., *Olaparib maintenance therapy in patients with newly diagnosed advanced ovarian cancer and a BRCA1 and/or BRCA2 mutation: SOLO1 China cohort.* Gynecol Oncol, 2021. **160**(1): p. 175-181.

78.   Miller, R.E., et al., *ESMO recommendations on predictive biomarker testing for homologous recombination deficiency and PARP inhibitor benefit in ovarian cancer.* Ann Oncol, 2020. **31**(12): p. 1606-1622.

79. Haunschild, C.E. and K.S. Tewari, *The current landscape of molecular profiling in the treatment of epithelial ovarian cancer.* Gynecol Oncol, 2021. **160**(1): p. 333-345.

80. Stover, E.H., et al., *Clinical assays for assessment of homologous recombination DNA repair deficiency.* Gynecol Oncol, 2020. **159**(3): p. 887-898.

81. Almeida, G.S., et al., *PARP inhibitor rucaparib induces changes in NAD levels in cells and liver tissues as assessed by MRS.* NMR Biomed, 2017. **30**(9).

82. Murai, J., et al., *Trapping of PARP1 and PARP2 by Clinical PARP Inhibitors.* Cancer Res, 2012. **72**(21): p. 5588-99.

83. Oza, A.M., et al., *Antitumor activity and safety of the PARP inhibitor rucaparib in patients with high-grade ovarian carcinoma and a germline or somatic BRCA1 or BRCA2 mutation: Integrated analysis of data from Study 10 and ARIEL2.* Gynecol Oncol, 2017. **147**(2): p. 267-275.

84. Penson, R.T., et al., *Olaparib monotherapy versus (vs) chemotherapy for germline BRCA-mutated (gBRCAm) platinum-sensitive relapsed ovarian cancer (PSR OC) patients (pts): Phase III SOLO3 trial.* Journal of Clinical Oncology, 2019. **37**(15_suppl): p. 5506-5506.

85. Shen, Y., et al., *BMN 673, a novel and highly potent PARP1/2 inhibitor for the treatment of human cancers with DNA repair deficiency.* Clin Cancer Res, 2013. **19**(18): p. 5003-15.

86. Murai, J., et al., *Stereospecific PARP trapping by BMN 673 and comparison with olaparib and rucaparib.* Mol Cancer Ther, 2014. **13**(2): p. 433-43.

87. Konecny, G.E. and R.S. Kristeleit, *PARP inhibitors for BRCA1/2-mutated and sporadic ovarian cancer: current practice and future directions.* Br J Cancer, 2016. **115**(10): p. 1157-1173.

88. Pommier, Y., M.J. O'Connor, and J. de Bono, *Laying a trap to kill cancer cells: PARP inhibitors and their mechanisms of action.* Sci Transl Med, 2016. **8**(362): p. 362ps17.

89. Siegel, R.L., K.D. Miller, and A. Jemal, *Cancer statistics, 2019.* CA: a cancer journal for clinicians, 2019. **69**(1): p. 7-34.

90. Vaughan, S., et al., *Rethinking ovarian cancer: recommendations for improving outcomes.* Nat Rev Cancer, 2011. **11**(10): p. 719-25.

91. Torre, L.A., et al., *Ovarian cancer statistics, 2018.* CA Cancer J Clin, 2018. **68**(4): p. 284-296.

92. Javle, M. and N.J. Curtin, *The role of PARP in DNA repair and its therapeutic exploitation.* Br J Cancer, 2011. **105**(8): p. 1114-22.

93. Bahena-González, A., A. Toledo-Leyva, and D. Gallardo-Rincón, *PARP inhibitors in ovarian cancer: evidence for maintenance and treatment strategies.* Chinese Clinical Oncology, 2020. **9**(4): p. 51.

94. Hong, T., et al., *PARP inhibition promotes ferroptosis via repressing SLC7A11 and synergizes with ferroptosis inducers in BRCA-proficient ovarian cancer.* Redox Biol, 2021. **42**: p. 101928.

95. Gelmon, K.A., et al., *Olaparib in patients with recurrent high-grade serous or poorly differentiated ovarian carcinoma or triple-negative breast cancer: a phase*

2, multicentre, open-label, non-randomised study. Lancet Oncol, 2011. **12**(9): p. 852-61.

96. Bowtell, D.D., et al., *Rethinking ovarian cancer II: reducing mortality from high-grade serous ovarian cancer.* Nat Rev Cancer, 2015. **15**(11): p. 668-79.

97. Musella, A., et al., *Rucaparib: An emerging parp inhibitor for treatment of recurrent ovarian cancer.* Cancer Treat Rev, 2018. **66**: p. 7-14.

98. Sandhu, S.K., et al., *The poly(ADP-ribose) polymerase inhibitor niraparib (MK4827) in BRCA mutation carriers and patients with sporadic cancer: a phase 1 dose-escalation trial.* Lancet Oncol, 2013. **14**(9): p. 882-92.

99. Moore, K., et al., *Maintenance Olaparib in Patients with Newly Diagnosed Advanced Ovarian Cancer.* N Engl J Med, 2018. **379**(26): p. 2495-2505.

100. Konstantinopoulos, P.A., et al., *Homologous Recombination Deficiency: Exploiting the Fundamental Vulnerability of Ovarian Cancer.* Cancer Discov, 2015. **5**(11): p. 1137-54.

101. Li, X., et al., *Disposition and drug-drug interaction potential of veliparib (ABT-888), a novel and potent inhibitor of poly(ADP-ribose) polymerase.* Drug Metab Dispos, 2011. **39**(7): p. 1161-9.

102. Jaspers, J.E., et al., *Loss of 53BP1 causes PARP inhibitor resistance in Brca1-mutated mouse mammary tumors.* Cancer Discov, 2013. **3**(1): p. 68-81.

103. Vaidyanathan, A., et al., *ABCB1 (MDR1) induction defines a common resistance mechanism in paclitaxel- and olaparib-resistant ovarian cancer cells.* Br J Cancer, 2016. **115**(4): p. 431-41.

104.   Aoki, S., et al., *Reversing effect of agosterol A, a spongean sterol acetate, on multidrug resistance in human carcinoma cells.* Jpn J Cancer Res, 2001. **92**(8): p. 886-95.

105.   Lei, Z.N., et al., *Establishment and Characterization of a Topotecan Resistant Non-small Cell Lung Cancer NCI-H460/TPT10 Cell Line.* Front Cell Dev Biol, 2020. **8**: p. 607275.

106.   Zhang, Y.K., et al., *Semi-synthetic ocotillol analogues as selective ABCB1-mediated drug resistance reversal agents.* Oncotarget, 2015. **6**(27): p. 24277-90.

107.   Fan, Y.F., et al., *Dacomitinib antagonizes multidrug resistance (MDR) in cancer cells by inhibiting the efflux activity of ABCB1 and ABCG2 transporters.* Cancer Lett, 2018. **421**: p. 186-198.

108.   Chen, X.Y., et al., *Overexpression of ABCC1 Confers Drug Resistance to Betulin.* Front Oncol, 2021. **11**: p. 640656.

109.   Johnson, Z.L. and J. Chen, *Structural Basis of Substrate Recognition by the Multidrug Resistance Protein MRP1.* Cell, 2017. **168**(6): p. 1075-1085.e9.

110.   Orlando, B.J. and M. Liao, *ABCG2 transports anticancer drugs via a closed-to-open switch.* Nat Commun, 2020. **11**(1): p. 2264.

111.   Trott, O. and A.J. Olson, *AutoDock Vina: improving the speed and accuracy of docking with a new scoring function, efficient optimization, and multithreading.* J Comput Chem, 2010. **31**(2): p. 455-61.

112.   Tariq, M., et al., *Liquid Chromatographic Method for Irinotecan Estimation: Screening of P-gp Modulators.* Indian J Pharm Sci, 2015. **77**(1): p. 14-23.

113. Tiwari, A.K., et al., *Nilotinib potentiates anticancer drug sensitivity in murine ABCB1-, ABCG2-, and ABCC10-multidrug resistance xenograft models.* Cancer Lett, 2013. **328**(2): p. 307-17.

114. Antolín, A.A. and J. Mestres, *Linking off-target kinase pharmacology to the differential cellular effects observed among PARP inhibitors.* Oncotarget, 2014. **5**(10): p. 3023-8.

115. Robey, R.W., et al., *Mutations at amino-acid 482 in the ABCG2 gene affect substrate and antagonist specificity.* Br J Cancer, 2003. **89**(10): p. 1971-8.

116. Alqawi, O., S. Bates, and E. Georges, *Arginine482 to threonine mutation in the breast cancer resistance protein ABCG2 inhibits rhodamine 123 transport while increasing binding.* Biochem J, 2004. **382**(Pt 2): p. 711-6.

117. Ejendal, K.F., et al., *The nature of amino acid 482 of human ABCG2 affects substrate transport and ATP hydrolysis but not substrate binding.* Protein Sci, 2006. **15**(7): p. 1597-607.

118. Honjo, Y., et al., *Acquired mutations in the MXR/BCRP/ABCP gene alter substrate specificity in MXR/BCRP/ABCP-overexpressing cells.* Cancer Res, 2001. **61**(18): p. 6635-9.

119. Dai, C.L., et al., *Lapatinib (Tykerb, GW572016) reverses multidrug resistance in cancer cells by inhibiting the activity of ATP-binding cassette subfamily B member 1 and G member 2.* Cancer Res, 2008. **68**(19): p. 7905-14.

120. Eadie, L.N., T.P. Hughes, and D.L. White, *Interaction of the efflux transporters ABCB1 and ABCG2 with imatinib, nilotinib, and dasatinib.* Clin Pharmacol Ther, 2014. **95**(3): p. 294-306.

121. Wu, Z.X., et al., *Tivantinib, A c-Met Inhibitor in Clinical Trials, Is Susceptible to ABCG2-Mediated Drug Resistance.* Cancers (Basel), 2020. **12**(1).

122. Heyes, N., P. Kapoor, and I.D. Kerr, *Polymorphisms of the Multidrug Pump ABCG2: A Systematic Review of Their Effect on Protein Expression, Function, and Drug Pharmacokinetics.* Drug Metab Dispos, 2018. **46**(12): p. 1886-1899.

123. Asghar, W., et al., *Engineering cancer microenvironments for in vitro 3-D tumor models.* Mater Today (Kidlington), 2015. **18**(10): p. 539-553.

124. Li, X., et al., *High PARP-1 expression predicts poor survival in acute myeloid leukemia and PARP-1 inhibitor and SAHA-bendamustine hybrid inhibitor combination treatment synergistically enhances anti-tumor effects.* EBioMedicine, 2018. **38**: p. 47-56.

125. Nieborowska-Skorska, M., et al., *Ruxolitinib-induced defects in DNA repair cause sensitivity to PARP inhibitors in myeloproliferative neoplasms.* Blood, 2017. **130**(26): p. 2848-2859.

126. Nozaki, M., et al., *Cysteinyl leukotriene receptor antagonists inhibit tumor metastasis by inhibiting capillary permeability.* Keio J Med, 2010. **59**(1): p. 10-8.

127. Shen, Y., et al., *The Effects of Combined Therapeutic Protocol on Allergic Rhinitis Symptoms and Molecular Determinants.* Iran J Allergy Asthma Immunol, 2022. **21**(2): p. 141-150.

128. Wu, T. and Y. Dai, *Tumor microenvironment and therapeutic response.* Cancer Lett, 2017. **387**: p. 61-68.

129. Hinshaw, D.C. and L.A. Shevde, *The Tumor Microenvironment Innately Modulates Cancer Progression.* Cancer Res, 2019. **79**(18): p. 4557-4566.

130. Assaraf, Y.G., et al., *The multi-factorial nature of clinical multidrug resistance in cancer.* Drug Resist Updat, 2019. **46**: p. 100645.

Vita

Name	*Qiuxu Teng*
Baccalaureate Degree	*Bachelor of Science, China Pharmaceutical University, Nanjing, China Major:Marine Pharmacology*
Date Graduated	*June, 2015*
Other Degrees and Certificates	*Master of Science, St. John's University, Major: Pharmacology*
Date Graduated	*September, 2018*